Journal of Medicinal Chemistry

Article

pubs.acs.org/jmc

Rapid Discovery of Highly Potent and Selective Inhibitors of Histone Deacetylase 8 Using Click Chemistry to Generate Candidate Libraries

Takayoshi Suzuki,*[,†,‡] Yosuke Ota,[§] Masaki Ri,[∥] Masashige Bando,[⊥] Aogu Gotoh,[†,§] Yukihiro Itoh,[†] Hiroki Tsumoto,[§] Prima R. Tatum,[§] Tamio Mizukami,[#] Hidehiko Nakagawa,[§] Shinsuke Iida,[∥] Ryuzo Ueda,[∥] Katsuhiko Shirahige,[⊥] and Naoki Miyata*[,§]

[†]Graduate School of Medical Science, Kyoto Prefectural University of Medicine, 13 Taishogun Nishitakatsukasa-Cho, Kita-ku, Kyoto 403-8334, Japan

[‡]PRESTO, Japan Science and Technology Agency (JST), 4-1-8 Honcho Kawaguchi, Saitama 332-0012, Japan

[§]Graduate School of Pharmaceutical Sciences, Nagoya City University, 3-1 Tanabe-dori, Mizuho-ku, Nagoya, Aichi 467-8603, Japan

[∥]Graduate School of Medical Sciences, Nagoya City University, 1 Kawasumi, Mizuho-cho, Mizuho-ku, Nagoya, Aichi 467-8601, Japan

[⊥]Institute of Molecular and Cellular Biosciences, the University of Tokyo, 1-1-1 Yayoi, Bunkyo-ku, Tokyo 113-0032, Japan

[#]Graduate School of Bio-Science, Nagahama Institute of Bio-Science and Technology, 1266 Tamura-cho, Nagahama, Shiga, 526-0829, Japan

Supporting Information

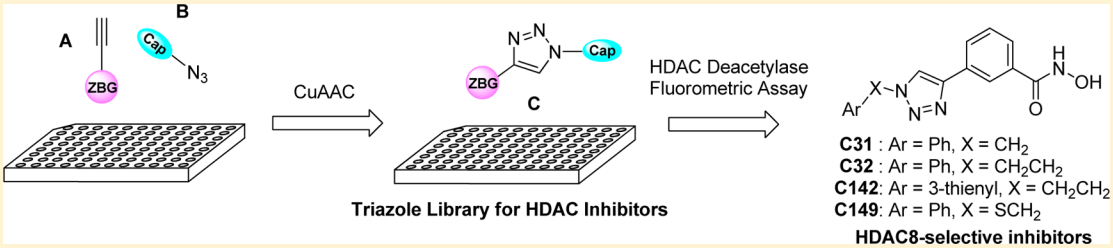

ABSTRACT: To find HDAC8-selective inhibitors, we designed a library of HDAC inhibitor candidates, each containing a zinc-binding group that coordinates with the active-site zinc ion, linked via a triazole moiety to a capping structure that interacts with residues on the rim of the active site. These compounds were synthesized by using click chemistry. Screening identified HDAC8-selective inhibitors including **C149** (IC_{50} = 0.070 μM), which was more potent than PCI-34058 (**6**) (IC_{50} = 0.31 μM), a known HDAC8 inhibitor. Molecular modeling suggested that the phenylthiomethyl group of **C149** binds to a unique hydrophobic pocket of HDAC8, and the orientation of the phenylthiomethyl and hydroxamate moieties (fixed by the triazole moiety) is important for the potency and selectivity. The inhibitors caused selective acetylation of cohesin in cells and exerted growth-inhibitory effects on T-cell lymphoma and neuroblastoma cells (GI_{50} = 3−80 μM). These findings suggest that HDAC8-selective inhibitors have potential as anticancer agents.

INTRODUCTION

Reversible acetylation/deacetylation of the ε-amino groups of lysine residues on histones and nonhistone proteins, catalyzed by histone acetyltransferases and histone deacetylases (HDACs), is involved in various life phenomena such as gene expression and cell cycle regulation.[1] Thus far, 18 HDAC family members have been identified and categorized into two groups, namely zinc-dependent enzymes (HDAC1−11) and NAD^+-dependent sirtuins (SIRT1−7).[2] Among them, HDAC8 is expressed tissue specifically and is localized in the nucleus[3] or cytoplasm.[4] It is responsible for genetic repression in acute myeloid leukemia[5] and is associated with the actin cytoskeleton in smooth muscle cells.[6] Furthermore, recent studies have revealed that HDAC8 is associated with several disease states. Gallimari et al. reported that siRNA targeting HDAC8 showed antitumor effects in cell culture.[7] Balasubramanian et al. reported that inhibition of HDAC8 induced apoptosis in T-cell lymphomas.[8] In addition, Oehme et al. suggested that HDAC8 is implicated in neuroblastoma tumorigenesis.[9] Therefore, HDAC8-selective inhibitors are of great interest, not only as tools for probing the biological functions of this isozyme but also as candidate anticancer agents having few side effects.

Although many HDAC inhibitors have been found so far,[10] including trichostatin A (TSA, **1**),[11] vorinostat (**2**),[12] and MS-275 (**3**)[13] (Chart 1), most lack HDAC8 selectivity. It has been reported that HDAC8 is selectively inhibited by SB-379278A (**4**),[14] linkerless hydroxamic acid **5**,[15] PCI-34051 (**6**),[8] azetidinone **7**,[16] and A8B4 (**8**) (Chart 2).[17] Among these compounds, compound **6** is a representative HDAC8-selective

Received: June 14, 2012
Published: November 1, 2012

Chart 1. Examples of HDAC Inhibitors

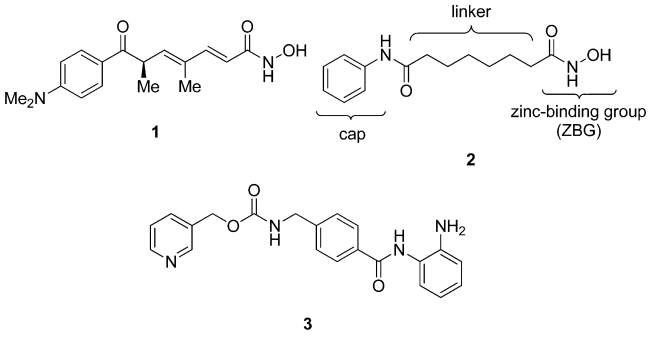

inhibitor that shows high potency and selectivity for HDAC8 over HDAC1, 2, 3, 6, and 10.

Chart 2. HDAC8-Selective Inhibitors

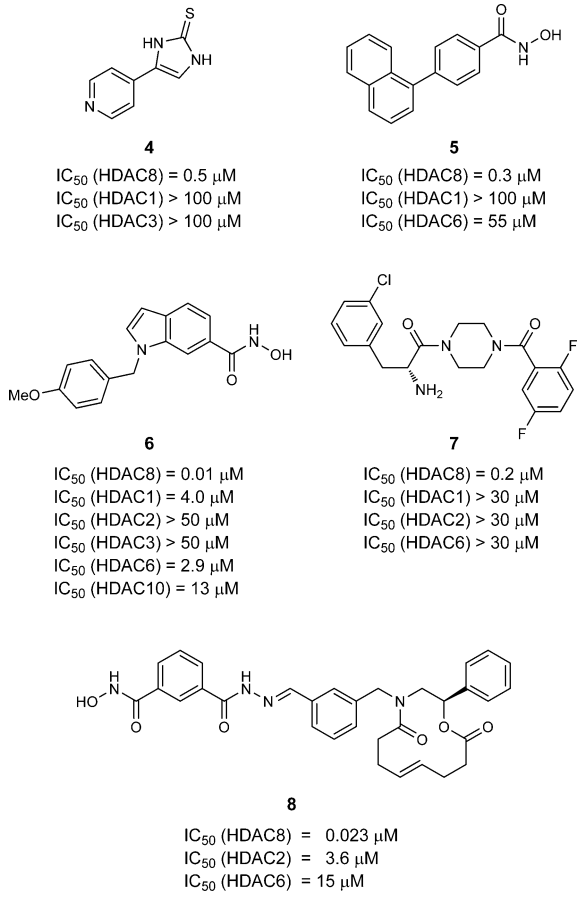

Various strategies have been employed to identify HDAC8-selective inhibitors to date. Compound **4** was identified by the evaluation of a chemical compound collection using an HDAC8 enzyme-based high-throughput screening,[14] and compounds **5**–**7** were discovered by drug design based on the crystal structure of HDAC8.[8,15,16] Here, we report the rapid identification of highly potent and selective inhibitors of HDAC8 by the use of Cu (I)-catalyzed azide–alkyne cycloaddition, a representative reaction in click chemistry,[18] to generate a library of candidates. Although several groups have used click chemistry to find HDAC inhibitors,[19] there has been no previous report on the use of click chemistry for the discovery of isozyme-selective HDAC inhibitors.

Chemistry. The routes used for the synthesis of the compounds prepared for this study are shown in Schemes 1–11.

Scheme 1. Synthesis of Alkyne A1[a]

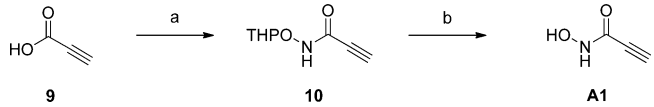

[a]Reagents and conditions: (a) NH_2OTHP, DCC, CH_2Cl_2, 0 °C to rt, 57%; (b) *p*-TsOH·H_2O, MeOH, rt, 70%.

The preparation of alkyne **A1** is shown in Scheme 1. Propiolic acid **9** was reacted with NH_2OTHP in the presence of DCC to give the corresponding *O*-THP hydroxamate **10**. Deprotection of the THP group of **10** by *p*-TsOH afforded **A1**. The preparation of alkyne **A2** (Scheme 2) started with 5-bromothiophene-2-carboxylic acid **11**, which was esterified and subjected to Sonogashira cross coupling with trimethylsilylacetylene to give **13**. Hydrolysis and EDCI/HOBt-mediated coupling with NH_2OTHP afforded the corresponding hydroxamate **15**, which provided **A2** upon removal of the THP group with *p*-TsOH. Compounds **A3** and **A4** were prepared from carboxylic acids **16a** and **16b** by using the same procedure described for the synthesis of **A2** (Scheme 3). *o*-Aminoanilides **A5**–**A8** were obtained by the condensation of 1,2-phenylenediamine with an appropriate carboxylic acid in the presence of condensing reagents (Scheme 4).

Azides **B2**–**B9**, **B11**, **B12**, and **B14** were prepared by azide displacement (NaN_3, DMSO) of the corresponding alkyl halides **21** (Scheme 5). Scheme 6 shows the synthesis of azides **B13** and **B15** from alcohols **22a** and **22b** via the tosylates **23a,b**. Azide **B10** was accessed from carboxylic acid **24** by $LiAlH_4$ reduction and alcohol-to-azide conversion using DPPA and DBU (Scheme 7). Phenethyl azide analogues **B16**–**B34** and **B36** were synthesized by azide displacement of the corresponding alkyl bromides **26** (Scheme 8). Scheme 9 shows the preparation of azides **B35** and **B37**–**B43** with an ethylene chain from alcohols **27** via the mesylate, bromide, or tosylates **28**. 1-Phenylethanone-2-azide **B45** and (*E*)-(2-azidovinyl)-benzene **B46** were prepared by azide displacement of the bromide **29** and the boronic acid **30**, respectively (Scheme 10).

Cu-catalyzed coupling of alkyne **A3** and azide **B1**, **B2**, **B37**, or **B44** provided triazoles **C31**, **C32**, **C142**, and **C149** (Scheme 11).

RESULTS AND DISCUSSION

Click Chemistry Approach. Fragment-based assembly is a drug discovery approach that enables high-throughput identification of small-molecular inhibitors using a minimal number of compounds as building blocks.[20] It allows medicinal chemists to explore $n \times m$ possibilities with $n + m$ combinations. Click chemistry is a powerful fragment-based assembly method and was shown to be highly versatile and effective for rapid synthesis/assembly of libraries of small molecules directed against a number of enzymes.[21] As reported before, triazole synthesis by Cu(I)-catalyzed azide–alkyne cycloaddition (CuAAC),[22] a key reaction in click chemistry, can provide a library of triazole-containing compounds, which are pure enough to be evaluated by means of in vitro assay without purification.

dx.doi.org/10.1021/jm300837y | J. Med. Chem. 2012, 55, 9562–9575

Scheme 2. Synthesis of Alkyne A2[a]

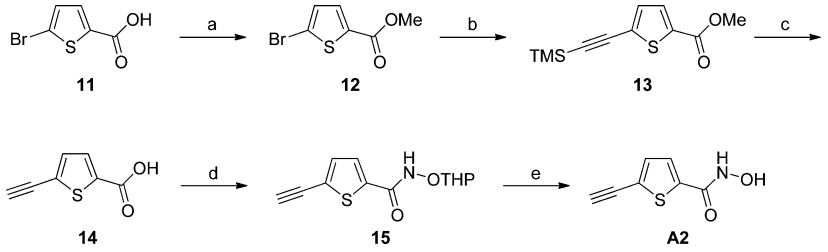

[a]Reagents and conditions: (a) conc H_2SO_4, MeOH, reflux, 96%; (b) trimethylsilylacetylene, $Pd(PPh_3)_2Cl_2$, CuI, Et_2NH, rt, 81%; (c) NaOH, H_2O, MeOH, rt, 97%; (d) NH_2OTHP, EDCI, HOBt·H_2O, DMF, rt, 90%; (e) *p*-TsOH·H_2O, MeOH, rt, 77%.

Scheme 3. Synthesis of Alkynes A3 and A4[a]

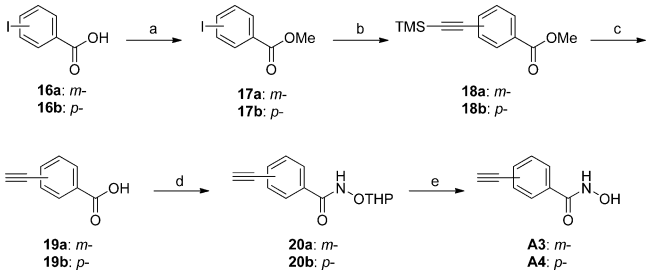

[a]Reagents and conditions: (a) conc H_2SO_4, MeOH, reflux, 96% for **17a**, 99% for **17b**; (b) trimethylsilylacetylene, $Pd(PPh_3)_2Cl_2$, CuI, Et_3N, THF, rt, 90% for **18a**, 64% for **18b**; (c) 2 N NaOH, MeOH, rt, 99% for **19a**, 92% for **19b**; (d) NH_2OTHP, EDCI, HOBt·H_2O, DMF, rt, 93% for **20a**, 86% for **20b**; (e) *p*-TsOH·H_2O, MeOH, rt, 86% for **A3**, 94% for **A4**.

Scheme 4. Synthesis of Alkynes A5–A8[a]

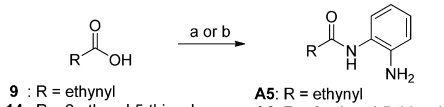

9 : R = ethynyl
14 : R = 2-ethynyl-5-thienyl
18a: R = 3-ethynylphenyl
18b: R = 4-ethynylphenyl

A5: R = ethynyl
A6: R = 2-ethynyl-5-thienyl
A7: R = 3-ethynylphenyl
A8: R = 4-ethynylphenyl

[a]Reagents and conditions: (a) 1,2-phenylenediamine, DCC, CH_2Cl_2, 0 °C to rt, 44% for **A5**; (b) 1,2-phenylenediamine, EDCI, HOBt·H_2O, DMF, rt, 79% for **A6**, 91% for **A7**, 86% for **A8**.

Scheme 5. Synthesis of Azides B2–B9, B11, B12, and B14[a]

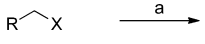

21a: R = CH_2Ph, X = Br
21b: R = $(CH_2)_2Ph$, X = Br
21c: R = $(CH_2)_3Ph$, X = Br
21d: R = $(CH_2)_4Ph$, X = Br
21e: R = 4-methoxyphenyl, X = Br
21f: R = 3-biphenyl, X = Br
21g: R = 4-biphenyl, X = Br
21h: R = 3-phenoxyphenyl, X = Cl
21i: R = 1-naphthyl, X = Cl
21j: R = 2-naphthyl, X = Br
21k: R = cyclohexyl, X = Br

B2: R = CH_2Ph
B3: R = $(CH_2)_2Ph$
B4: R = $(CH_2)_3Ph$
B5: R = $(CH_2)_4Ph$
B6: R = 4-methoxyphenyl
B7: R = 3-biphenyl
B8: R = 4-biphenyl
B9: R = 3-phenoxyphenyl
B11: R = 1-naphthyl
B12: R = 2-naphthyl
B14: R = cyclohexyl

[a]Reagents and conditions: (a) NaN_3, DMSO, rt or 80 °C, 21–92%.

In general, the pharmacophore for HDAC inhibitors consists of a zinc-binding group (ZBG) that coordinates with the zinc ion in the active site, a capping structure that interacts with residues on the rim of the active site, and a linker connecting the cap part and the ZBG with an appropriate separation. For example, compound **2** (Chart 1), a clinically used HDAC

Scheme 6. Synthesis of Azides B13 and B15[a]

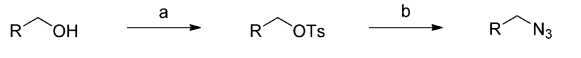

22a: R = cyclopentyl
22b: R = 1-adamantyl

23a: R = cyclopentyl
23b: R = 1-adamantyl

B13: R = cyclopentyl
B15: R = 1-adamantyl

[a]Reagents and conditions: (a) TsCl, pyridine, rt, 68% for **23a**, 84% for **23b**; (b) NaN_3, DMSO, 80 °C, 26% for **B13**, 84% for **B15**.

Scheme 7. Synthesis of Azide B10[a]

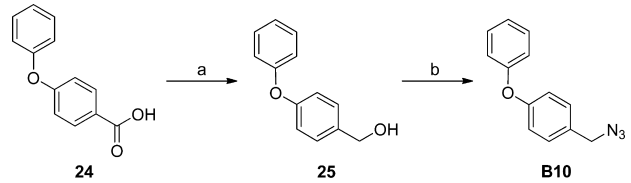

[a]Reagents and conditions: (a) $LiAlH_4$, THF, 0–80 °C, 87%; (b) DPPA, DBU, DMF, rt, 30%.

Scheme 8. Synthesis of Azides B16–B34 and B36[a]

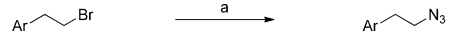

26a: Ar = 2-Me-Ph
26b: Ar = 3-Me-Ph
26c: Ar = 4-Me-Ph
26d: Ar = 2-OMe-Ph
26e: Ar = 3-OMe-Ph
26f: Ar = 4-OMe-Ph
26g: Ar = 2-Cl-Ph
26h: Ar = 3-Cl-Ph
26i: Ar = 4-Cl-Ph
26j: Ar = 2-F-Ph
26k: Ar =3-F-Ph
26l: Ar =4-F-Ph
26m:Ar =2-CF_3-Ph
26n: Ar =3-CF_3-Ph
26o: Ar =4-CF_3-Ph
26p: Ar =2-NO_2-Ph
26q: Ar =3-NO_2-Ph
26r: Ar =4-NO_2-Ph
26s: Ar =1-naphthyl
26t: Ar =3-indolyl

B16: Ar = 2-Me-Ph
B17: Ar = 3-Me-Ph
B18: Ar = 4-Me-Ph
B19: Ar = 2-OMe-Ph
B20: Ar = 3-OMe-Ph
B21: Ar = 4-OMe-Ph
B22: Ar = 2-C-Ph
B23: Ar = 3-Cl-Ph
B24: Ar = 4-Cl-Ph
B25: Ar = 2-F-Ph
B26: Ar =3-F-Ph
B27: Ar =4-F-Ph
B28: Ar =2-CF_3-Ph
B29: Ar =3-CF_3-Ph
B30: Ar =4-CF_3-Ph
B31: Ar =2-NO_2-Ph
B32: Ar =3-NO_2-Ph
B33: Ar =4-NO_2-Ph
B34: Ar =1-naphthyl
B36: Ar =3-indolyl

[a]Reagents and conditions: (a) NaN_3, DMSO, rt or 80 °C, 62–100%.

inhibitor, consists of hydroxamic acid (ZBG), anilide (cap), and alkyl chain (linker). Accordingly, we designed a library of candidate HDAC inhibitors in which the ZBG and the cap group are connected by a triazole-containing linker (Figure 1).[19a] We designed various alkynes with hydroxamic acid (**A1**–**A4**) or *o*-aminoanilide (**A5**–**A8**) as the ZBG and azides with various cap structures (**B1**–**B15**) as suitable building blocks for click assembly to construct a structurally diverse chemical library that might provide a high hit rate. We then prepared eight alkynes **A1**–**A8** and 15 alkyl azides **B1**–**B15** as shown in Schemes 1–7. Using the CuAAC reaction, a 120-member HDAC inhibitor library was assembled in microtiter plates. Each of the eight alkynes was mixed with each of the 15 azides in DMSO solution, followed by the addition of catalytic amounts of $CuSO_4$, sodium ascorbate, and tris[(1-benzyl-1*H*-1,2,3-triazol-4-yl)methyl]amine (TBTA). The disappearance of the starting materials and the quantitative formation of the triazole products were confirmed by TLC and LC-MS

dx.doi.org/10.1021/jm300837y | J. Med. Chem. 2012, 55, 9562–9575

Scheme 9. Synthesis of Azides B35 and B37−B43[a]

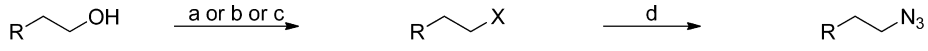

27a: R = 2-naphtyl	**28a**: R = 2-naphtyl, X = OMs	**B35**: 2-naphtyl
27b: R = 3-thienyl	**28b**: R = 3-thienyl, X = OMs	**B37**: 3-thienyl
27c: R = 2-pyridinyl	**28c**: R = 2-pyridinyl, X = Br	**B38**: 2-pyridinyl
27d: R = 4-methylthiazolyl	**28d**: R = 4-methylthiazolyl, X = OMs	**B39**: 4-methylthiazolyl
27e: R = 4-morpholinyl	**28e**: R = 4-morpholinyl, X = OMs	**B40**: 4-morpholinyl
27f: R = cyclopentyl	**28f**: R = cyclopentyl, X = OTs	**B41**: cyclopentyl
27g: R = cyclohexyl	**28g**: R = cyclohexyl, X =OTs	**B42**: cyclohexyl
27h: R = 1-adamantyl	**28h**: R = 1-adamantyl, X= OTs	**B43**: 1-adamantyl

[a]Reagents and conditions: (a) MsCl, Et_3N, CH_2Cl_2, rt; (b) TsCl, pyridine, rt; (c) CBr_4, PPh_3, CH_2Cl_2, rt; (d) NaN_3, DMSO, rt or 80 °C, 16−86% (two steps).

Scheme 10. Synthesis of Azides B45 and B46[a]

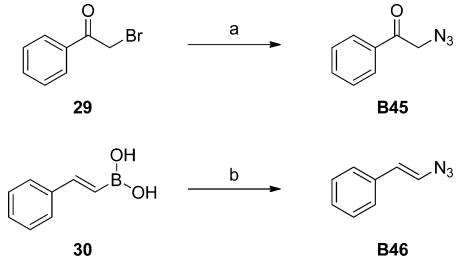

[a]Reagents and conditions: (a) NaN_3, DMSO, rt, 53%; (b) NaN_3, $CuSO_4$, MeOH, rt, 40%.

(Supporting Information Figure S1). The generated triazole compounds **C1−C120** are shown in Supporting Information Figure S2. The 120 triazoles could be directly screened for HDAC-inhibitory activity in the microtiter plates without further purification. To find HDAC8-selective inhibitors, compounds **C1−C120** were tested for activity against both HDAC8 at 0.3 μM and total HDACs from HeLa nuclear extracts at 3 μM. We chose total HDACs from HeLa nuclear extracts for primary screening because these extracts are rich in the activity of HDAC1 and HDAC2, which are major isozymes of the HDAC family.[23] In this HDAC8 assay, the HDAC8-inhibitory activity of compound **2** at 0.3 μM in the presence of 10 mol % Cu(I) was almost the same as that in the absence of Cu(I) (31.9 ± 0.12% inhibition in the presence of Cu(I), 35.0 ± 0.72% inhibition in the absence of Cu(I)), suggesting that Cu(I) does not affect the activity of compounds **C1−C120**. As shown in Figures 2 and 3, two hits emerged from these screens. The HDAC8-inhibitory activity of these two crude compounds **C31** and **C32** was comparable to that of compound **6** at 0.3 μM (Figure 2). Furthermore, at the concentration of 3 μM, crude **C31** and **C32** showed weak inhibitory activity against total HDACs from HeLa nuclear extract (Figure 3).

To identify HDAC8-selective inhibitors more potent than compound **6**, we further designed a **C32**-based library of compounds, which could be prepared from alkyne **A3** and azides **B16−B46** (Schemes 8−10) (Figure 4) using the same click chemistry approach. The CuAAC reaction between alkyne **A3** and azides **B16−B46** gave 31 triazoles **C121−C151**, which are structurally related to compound **C32** (Supporting Information Figure S3). The 31 triazole compounds were screened against both HDAC8 and total HDACs from HeLa nuclear extracts. Two crude compounds, **C142** and **C149**, showed more potent inhibition than **C32** at the concentration of 0.3 μM (Figure 5) while displaying weak inhibition toward HDACs from HeLa nuclear extracts at the concentration of 3 μM, indicating high selectivity for HDAC8 (Figure 6).

Isozyme Selectivity. Compounds **C31**, **C32**, **C142**, and **C149** were resynthesized and purified by column chromatography and recrystallization (Scheme 11). The pure compounds **C31**, **C32**, **C142**, and **C149** were evaluated for inhibitory effects on HDAC1, HDAC2, HDAC4, HDAC6, and HDAC8 as well as total HDACs from nuclear extracts. The results of the enzyme assays are shown in Table 1. In these assays, compound **6** inhibited HDAC8 with an IC_{50} of 0.31 μM and showed selectivity for HDAC8 over HDAC1, HDAC2, HDAC4, and HDAC6.

Compounds **C31**, **C32**, **C142**, and **C149** all showed potent HDAC8-inhibitory activity. The HDAC8-inhibitory activity of compounds **C31** and **C32** was greater than that of compound **2** and comparable to that of compound **6** (IC_{50} of **2** 1.5 μM, **6** 0.31 μM, **C31** 0.35 μM, **C32** 0.18 μM). Compounds **C142** and **C149**, which are derivatives of **C32**, showed more potent HDAC8-inhibitory activity than compound **6** (IC_{50} of **C142** 0.10 μM, **C149** 0.070 μM). Furthermore, while compound **2** inhibited HDAC1, HDAC2, and HDAC6 more potently than HDAC8, compounds **C31**, **C32**, **C142**, and **C149** inhibited HDAC8 in preference to the other isozymes, like compound **6**. Thus, **C31**, **C32**, **C142**, and **C149** are potent and selective inhibitors of HDAC8.

Scheme 11. Synthesis of HDAC8-Selective Inhibitors C31, C32, C142, and C149[a]

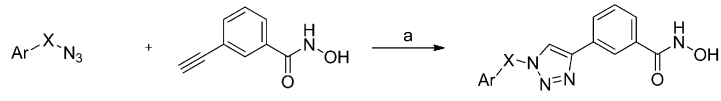

B1 : Ar = Ph, X = CH_2	**A3**	**C31** : Ar = Ph, X = CH_2
B2 : Ar = Ph, X = CH_2CH_2		**C32** : Ar = Ph, X = CH_2CH_2
B37: Ar = 3-thienyl, X = CH_2CH_2		**C142**: Ar = 3-thienyl, X = CH_2CH_2
B44: Ar = Ph, X = SCH_2		**C149**: Ar = Ph, X = SCH_2

[a]Reagents and conditions: (a) $CuSO_4·5H_2O$, sodium ascorbate, TBTA, MeOH, H_2O, rt, 92−100%.

dx.doi.org/10.1021/jm300837y | J. Med. Chem. 2012, 55, 9562−9575

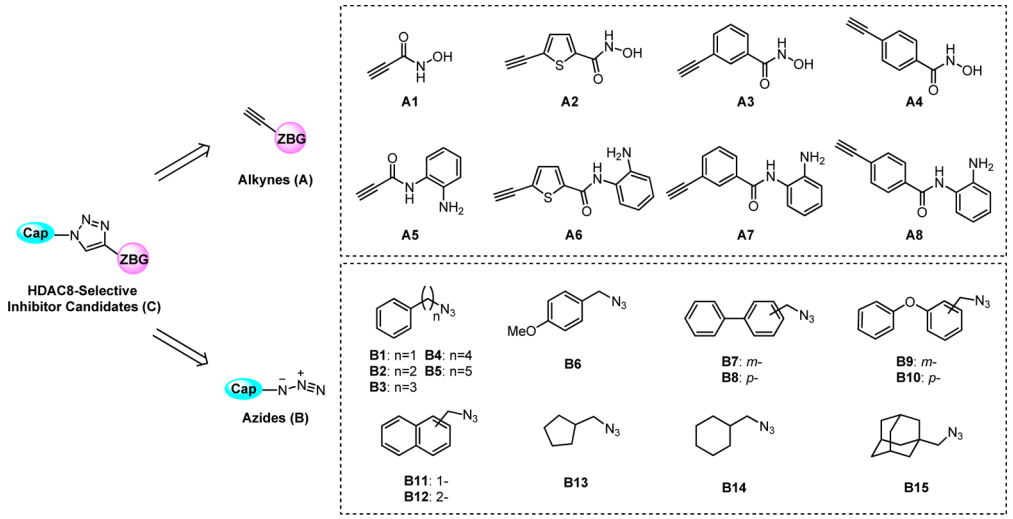

Figure 1. Design of alkynes and azides.

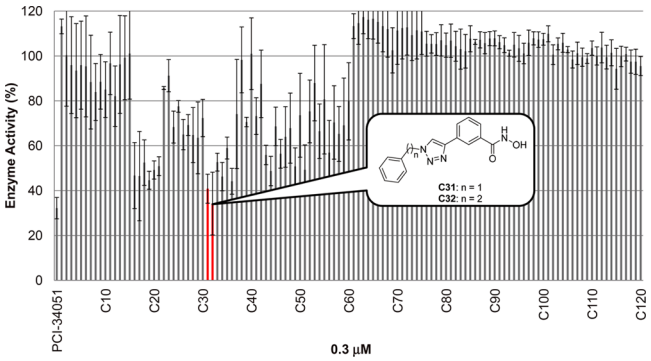

Figure 2. HDAC8 activity in the presence of 0.3 μM **C1**−**C120**.

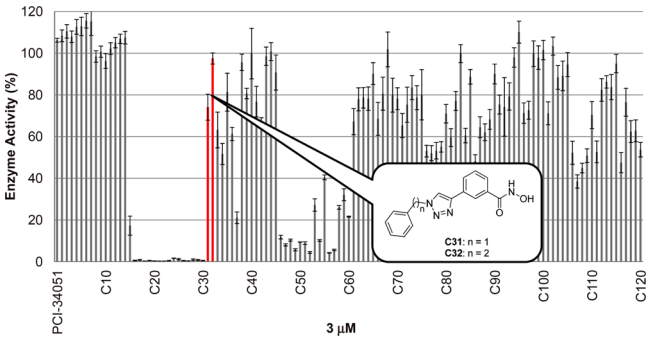

Figure 3. Total HDACs activity in the presence of 3 μM **C1**−**C120**.

Molecular Modeling. Although several X-ray crystal structures of HDAC8 have been reported,[16,23] we chose the crystal structure of HDAC8 complexed with CRA-A (PDB code 1VKG) for the molecular modeling study on compounds **6** and **C149** with HDAC8. Unlike the other structures, the HDAC8−CRA-A complex structure has a hydrophobic pocket which is thought to be unique to HDAC8.[15,23a] It is therefore reasonable to assume that HDAC8-selective inhibitors bind to this unique pocket. The lowest energy conformations of **6**, a previously reported HDAC8-selective inhibitor, and **C149**, the most active HDAC8-selective inhibitor in the present series, were obtained when they were docked into a model based on the crystal structure of HDAC8 (PDB code 1VKG), using the software packages Glide 3.5 and MacroModel 8.1 (Figures 7 and 8).

In the simulated HDAC8/compound **6** complex, the hydroxamate group of compound **6** coordinates in a bidentate fashion to the zinc ion and forms three hydrogen bonds with His 142, His 143, and Tyr 306 in the active center of HDAC8 (Figure 7). The 4-methoxybenzyl group of compound **6** is located in the unique hydrophobic pocket of HDAC8, where the CH of the methoxy group can interact with Tyr 154 via CH−π interaction. It is also suggested that the indole ring of compound **6** orients the hydroxamate group and 4-methoxybenzyl group into the appropriate geometry.

Inspection of the simulated HDAC8/compound **C149** complex showed that the hydroxamic acid group coordinates the zinc ion through its CO and OH groups in a similar way to compound **6**. It is also suggested that the hydroxamate group of **C149** forms a hydrogen bond between its CO moiety and His 142 and also forms another hydrogen bond between its OH moiety and Tyr 306 (Figure 8). Unlike compound **6**, it is suggested that **C149** has a U-shaped conformation in the active site of HDAC8, and most importantly, the phenylthiomethyl group of compound **C149** binds to a hydrophobic pocket formed by Trp 141, Ile 34, and Pro 35, which is thought to be unique to HDAC8 and where the methylthio group can interact with Trp 141 and the phenyl group can bind to Pro 35 and Tyr 306 through hydrophobic interactions. The three nitrogens of the triazole ring of **C149** do not appear to interact with any amino acid residues of HDAC8, but the triazole ring can interact with the methylene group of Phe 152 through CH−π or hydrophobic interactions (the distance between the CH_2 of Phe 152 and the triazole is 3.2 Å). The triazole ring is also considered to be important to fix the orientation of the zinc-binding hydroxamate and the hydrophobic pocket-binding phenylthiomethyl group appropriately, thereby contributing to the potent HDAC8-inhibitory activity and HDAC8-selectivity of compound **C149**. Comparison of the simulated HDAC8/inhibitor complex structures suggests that compound **C149** can bind to HDAC8 more tightly than can compound **6** through efficient hydrophobic interactions.

In addition, we attempted to carry out a docking study of compound **C149** to HDAC2 (PDB code 3MAX),[24] another HDAC isozyme. However, compound **C149** could not be docked in the active site of HDAC2 because of a steric clash

dx.doi.org/10.1021/jm300837y | J. Med. Chem. 2012, 55, 9562−9575

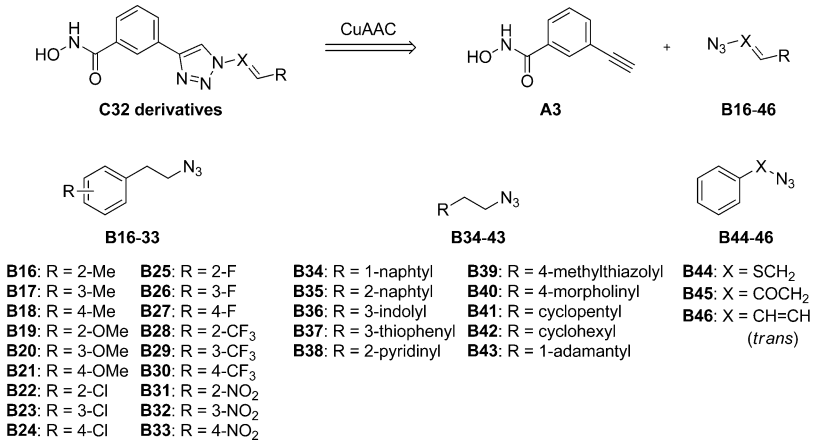

Figure 4. Design of a **C32**-based library of compounds.

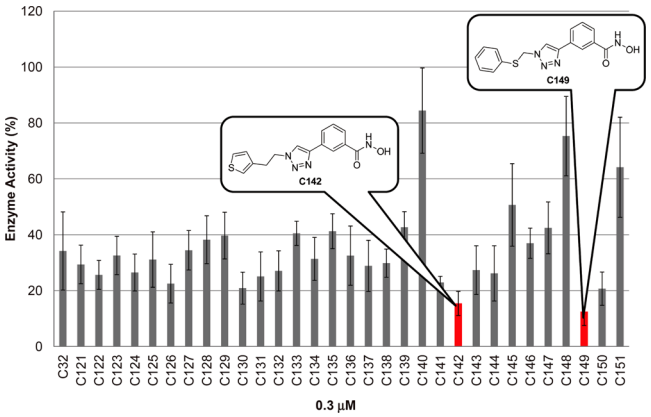

Figure 5. HDAC8 activity in the presence of 0.3 μM **C121**−**C151**.

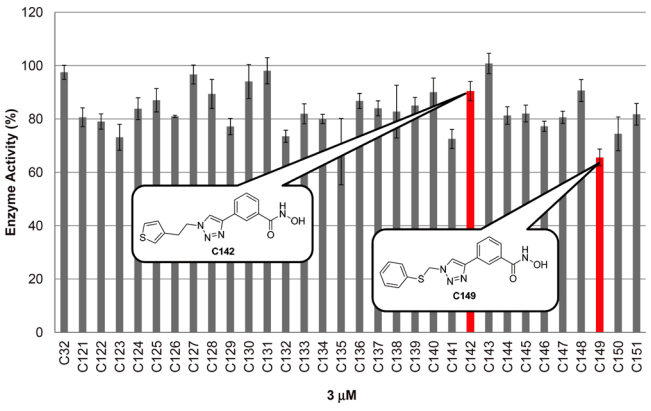

Figure 6. Total HDACs activity in the presence of 3 μM **C121**−**C151**.

between the phenylthiomethyl group of **C149** and the rim of the HDAC2 active site. These calculation results are consistent with the experimental fact that compound **C149** inhibits HDAC8 in preference to HDAC2 (Table 1).

Cellular Assays. Because HDAC8 is a cohesin deacetylase,[25] inhibition of HDAC8 and that of other HDACs can be assessed by evaluating accumulation of acetylated cohesin and acetylated histone, respectively, using Western blot analysis. Therefore, we examined the effects of compound **6**, **C142**, and **C149** on accumulation of acetylated cohesin and histone H4 (Figure 9). In accordance with the results of enzyme assays, compound **6** and compounds **C142** and **C149** produced a dose-dependent increase of cohesin acetylation without a major increase in acetylated H4. These results indicate that compounds **C142** and **C149** potently and selectively inhibit HDAC8 in preference to other HDACs in cells.

Because it has been reported that inhibition of HDAC8 induces apoptosis in T-cell lymphomas[8] and HDAC8 is implicated in neuroblastoma tumorigenesis,[9] compounds **6**, **C32**, and **C149** were tested in cell growth-inhibition assays using human T-cell lymphoma and neuroblastoma cell lines. The results are shown in Table 2. These HDAC8-selective inhibitors showed clear growth-inhibitory effects on both T-cell lymphoma and neuroblastoma cell lines, including Jurkat, HH, MT2, MT4, NB-1, and LA-N-1. In particular, the growth-inhibitory activity against T-cell lymphoma cells of compound **C149** was greater than that of compound **6**. It should be noted that these inhibitors did not affect the growth of healthy donor peripheral blood mononuclear cells (PBMCs) (IC_{50} values >100 μM), suggesting that the cytotoxicity of HDAC8-selective inhibitors is cell-type-specific. These results suggest that HDAC8 is involved in the growth of T-cell lymphoma and neuroblastoma cells and that our HDAC8-selective inhibitors may be useful in the treatment of T-cell lymphoma and neuroblastoma.

■ CONCLUSION

In summary, we used click chemistry with the reliable CuAAC reaction initially to prepare a triazole library of 120 compounds, among which two potent HDAC8 inhibitors **C31** and **C32** were identified. For further structural optimization, we next prepared a 31-member library based on the structure of compound **C32**. Screening led to the identification of two highly potent and selective HDAC8 inhibitors, **C142** and **C149**. A molecular modeling study of the HDAC8/**C149** complex suggested that the orientation of the hydrophobic pocket-binding phenylthiomethyl group and the zinc-binding hydroxamate, fixed by the triazole ring, is important for both HDAC8-inhibitory activity and HDAC8-selectivity. Compounds **C32** and **C149** also showed in-cell HDAC8 selectivity and potent T-cell lymphoma cell growth-inhibitory activity.

Thus, we have rapidly identified a novel series of HDAC8-selective inhibitors by using click chemistry to generate libraries of candidate molecules. It should be possible to obtain even more potent and selective HDAC8 inhibitors by means of further structural development. HDAC8-selective inhibitors are thought to have considerable potential both for the develop-

dx.doi.org/10.1021/jm300837y | J. Med. Chem. 2012, 55, 9562−9575

Table 1. HDAC-Inhibitory Activity of Compounds 2, 6, C31, C32, C142, and C149[a]

	IC_{50} (μM)					
	HDACs	class I		class IIa	class IIb	
compd	(nuclear extract)	HDAC1	HDAC2	HDAC8	HDAC4	HDAC6
2	0.17	0.27	0.78	1.5	>10	0.21
6	>100	>100	>100	0.31	>100	9.3
C31	37	41	65	0.35	30	7.9
C32	23	>100	76	0.18	>100	3.2
C142	44	>100	>100	0.10	>100	1.1
C149	54	38	>100	0.070	44	2.4

[a]Values are means of at least three experiments.

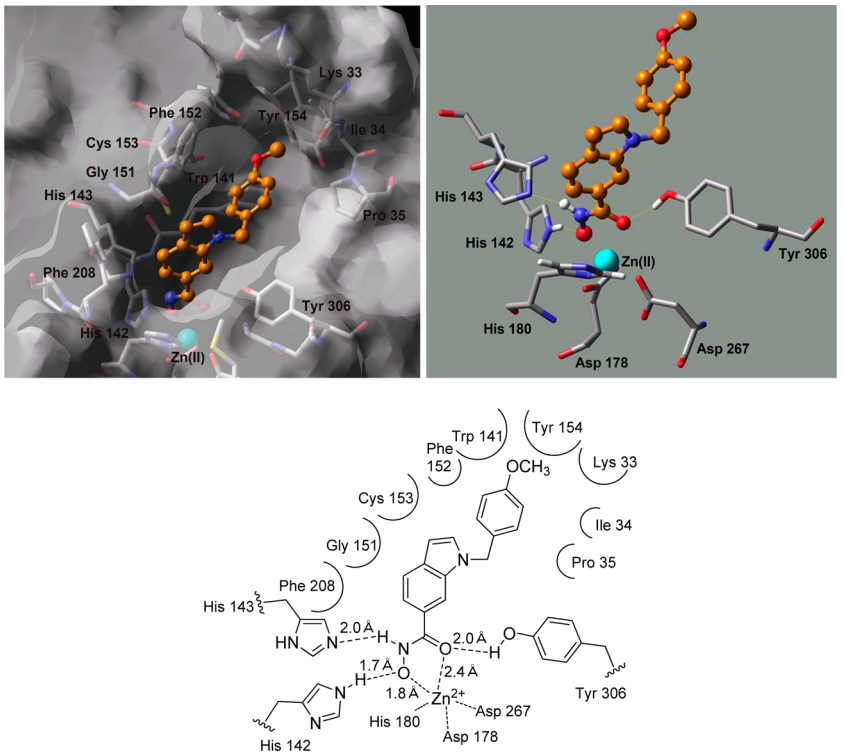

Figure 7. The lowest energy conformation of **6** (ball-and-stick representation) in the HDAC8 catalytic core. Compound **6** was docked into a model based on the crystal structure of HDAC8 (PDB code 1VKG), using the software packages Glide 3.5 and MacroModel 8.1. (top left) Surface view of **6** docked in the HDAC8 catalytic pocket. (top right) View of the catalytic center of HDAC8 complexed with **6**. Residues within 3 Å of the zinc ion are displayed. (bottom) Schematic representation of **6** binding with HDAC8.

ment of novel therapeutic agents and as tools for biological research.

EXPERIMENTAL SECTION

Chemistry. Melting points were determined using a Yanagimoto micro melting point apparatus or a Büchi 545 melting point apparatus and were left uncorrected. Proton nuclear magnetic resonance spectra (^{1}H NMR) and carbon nuclear magnetic resonance spectra (^{13}C NMR) were recorded in the indicated solvent on a JEOL JNM-LA500, JEOL JNM-A500, or BRUKER AVANCE600 spectrometer. Chemical shifts (δ) are reported in parts per million relative to the internal standard, tetramethylsilane. Elemental analysis was performed with a Yanaco CHN CORDER NT-5 analyzer, and all values were within ±0.4% of the calculated values, confirming >95% purity. High-resolution mass spectra (HRMS) and fast atom bombardment (FAB) mass spectra were recorded on a JEOL JMS-SX102A mass spectrometer. GC-MS analyses were performed on a Shimadzu GCMS-QP2010. IR spectra were measured on a Shimadzu FTIR-8400S spectrometer. LCMS was performed with a Waters instrument equipped with Unison US-C18 (2 mm × 5 mm/2 × 150 mm, Imtakt Corporation). Reagents and solvents were purchased from Aldrich, Tokyo Kasei Kogyo, Wako Pure Chemical Industries, and Kanto Kagaku and used without purification. Flash column chromatography was performed using silica gel 60 (particle size 0.046−0.063 mm) supplied by Merck.

Propynoic Acid Hydroxyamide (A1). *Step 1: Preparation of Propynoic Acid Tetrahydropyran-2-yloxyamide (**10**).* To a solution of propynoic acid (**9**, 300 mg, 4.28 mmol) in CH_2Cl_2 (6 mL) and NH_2OTHP (552 mg, 4.71 mmol) was added dropwise a solution of DCC (972 mg, 4.71 mmol) in CH_2Cl_2 (9 mL) at 0 °C. The reaction mixture was stirred for 3 h at room temperature. Filtration, concentration in vacuo, and purification of the residue by silica gel flash chromatography (AcOEt/*n*-hexane = 2/3) gave 416 mg (57%) of **10** as a pale-yellow oil. ^{1}H NMR ($CDCl_3$, 500 MHz, δ; ppm): 8.76 (1H, s), 5.01 (1H, s), 3.96 (1H, t, J = 10.2 Hz), 3.96−3.65 (1H, m), 2.89 (1H, s), 1.94−1.78 (3H, m), 1.71−1.61 (3H, m).

*Step 2: Preparation of Propynoic Acid Hydroxyamide (**A1**).* To a solution of **10** (416 mg, 2.46 mmol) obtained above in MeOH (21 mL) was added $TsOH{\cdot}H_2O$ (47 mg, 0.246 mmol). The reaction mixture was stirred for 30 h at room temperature. After removal of the solvent, the residue was purified by silica gel flash column

dx.doi.org/10.1021/jm300837y | J. Med. Chem. 2012, 55, 9562−9575

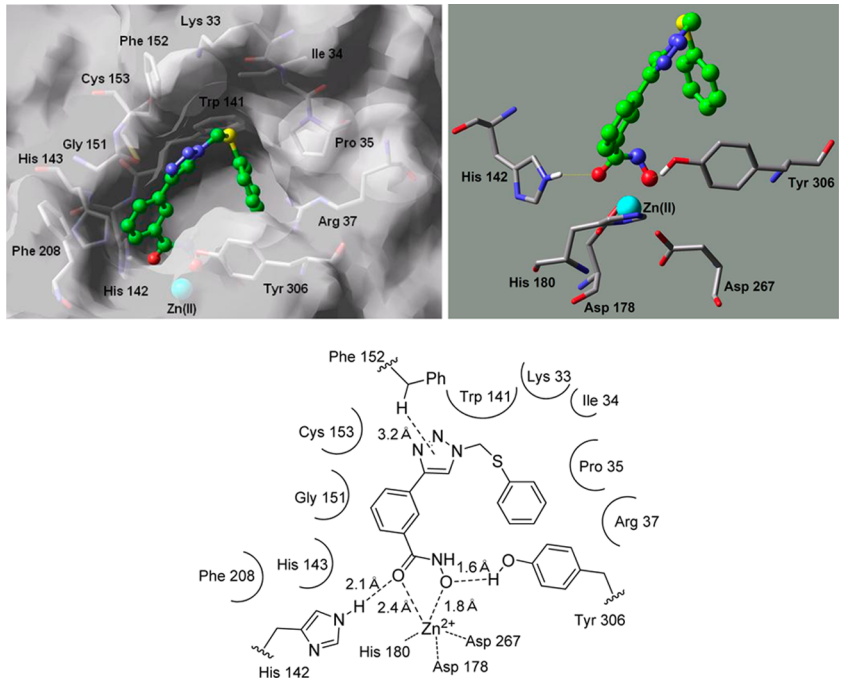

Figure 8. The lowest energy conformation of **C149** (ball-and-stick representation) in the HDAC8 catalytic core. Compound **C149** was docked into a model based on the crystal structure of HDAC8 (PDB code 1VKG), using the software packages Glide 3.5 and MacroModel 8.1. (top left) Surface view of **C149** docked in the HDAC8 catalytic pocket. (top right) View of the catalytic center of HDAC8 complexed with **C149**. Residues within 3 Å of the zinc ion are displayed. (bottom) Schematic representation of **C149** binding with HDAC8.

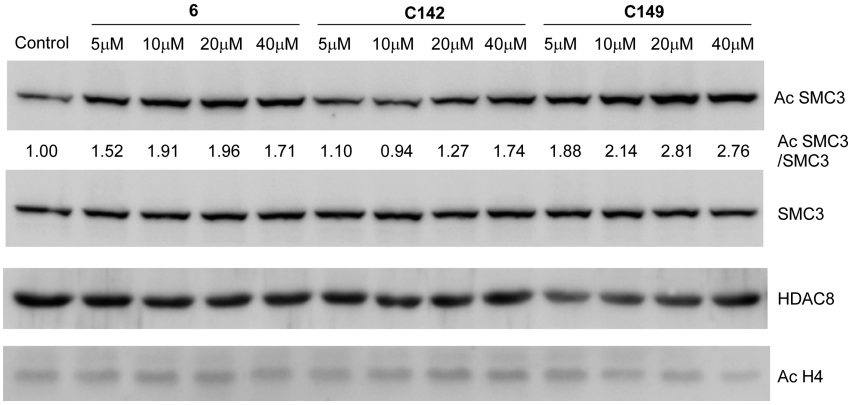

Figure 9. Western blot detection of acetylated structural maintenance of chromosome 3 (SMC3), a subunit of cohesin, and H4 levels in HeLa cells after 4 h treatment with compounds **6**, **C142**, and **C149**. Values of Ac SMC3/SMC3 ratio determined by optical density measurement of the blots are shown below the uppermost photograph.

chromatography (AcOEt/*n*-hexane = 3/1) to give 147 mg (70%) of **A1** as a white solid. The solid was recrystallized from AcOEt/*n*-hexane to give 70 mg of **A1** as colorless crystals; mp 69−71 °C. ^{1}H NMR (DMSO-d_6, 500 MHz, δ; ppm): 11.2 (1H, broad s), 9.28 (1H, s), 4.18 (1H, s). ^{13}C NMR (DMSO-d_6, 150 MHz, δ; ppm): 149.15, 77.32, 76.03. HRMS (EI) Calcd. for $C_3H_3O_2N$ 85.0160, Found 85.0159.

5-Ethynylthiophene-2-carboxylic Acid Hydroxyamide (A2). *Step 1: Preparation of 5-Bromothiophene-2-carboxylic Acid Methyl Ester (**12**).* To a solution of 5-bromo-2-thiophenecarboxylic acid (**11**, 1.00 g, 4.83 mmol) in MeOH (30 mL) was added concentrated H_2SO_4 (1.00 mL). The reaction mixture was refluxed for 30 h. After removal of the solvent, the residue was poured into water and extracted with AcOEt. The organic layer was separated, washed with brine, and dried over Na_2SO_4. Filtration, concentration in vacuo, and purification of the residue by silica gel flash column chromatography (AcOEt/*n*-hexane = 1/10) gave 1.03 g (96%) of **12** as a white solid. ^{1}H NMR ($CDCl_3$, 500 MHz, δ; ppm): 7.55 (1H, d, J = 4.0 Hz), 7.07 (1H, d, J = 4.0 Hz), 3.88 (3H, s).

*Step 2: Preparation of 5-Trimethylsilanylethynylthiophene-2-carboxylic Acid Methyl Ester (**13**).* To a solution of **12** (1.03 g, 4.66 mmol) obtained above, $PdCl_2(PPh_3)_2$ (32.7 mg, 46.6 μmol), and CuI (13.3 mg, 69.9 μmol) in diethylamine (15.5 mL) was added trimethylsilylacetylene (687 mg, 6.99 mmol). The mixture was stirred for 18 h at room temperature. After removal of the solvent, the residue was diluted with Et_2O and the Et_2O solution was washed with 1 N aqueous HCl, saturated $NaHCO_3$, and brine, and then dried over Na_2SO_4. Filtration, concentration in vacuo, and purification of the residue by silica gel flash column chromatography (AcOEt/*n*-hexane = 1/20) gave 895 mg (81%) of **13** as a brown solid. ^{1}H NMR ($CDCl_3$, 500 MHz, δ; ppm): 7.63 (1H, d, J = 4.0 Hz), 7.16 (1H, d, J = 4.0 Hz), 3.88 (3H, s), 0.257 (9H, s).

*Step 3: Preparation of 5-Ethynylthiophene-2-carboxylic Acid (**14**).* To a solution of **13** (895 mg, 3.75 mmol) obtained above in MeOH (10 mL) was added 2 N aqueous NaOH (3.75 mL, 7.50 mmol) at 0 °C. The reaction mixture was stirred for 5 h at room temperature. The mixture was acidified with 2 N aqueous HCl and

dx.doi.org/10.1021/jm300837y | J. Med. Chem. 2012, 55, 9562−9575

Table 2. Growth Inhibition of Various Cancer Cells by Compounds 6, C32, and C149[a]

cell type	cell line	GI_{50} (μM) 6	C32	C149
T-cell	Jurkat	11	11	7.6
	HH	>100	79	23
	MT2	15	19	11
	MT4	25	30	15
neuroblastoma cell	NB-1	14	39	12
	LA-N-1	3.9	27	6.4
healthy PBMC cell	PB-O	97	>100	>100
	PB-N	>100	>100	>100

[a]Values are means of at least three experiments.

concentrated in vacuo. The residue was diluted with AcOEt and the AcOEt solution was washed brine and dried over Na_2SO_4. Filtration and concentration in vacuo gave 552 mg (97%) of **14** as a brown solid. ^{1}H NMR (DMSO-d_6, 500 MHz, δ; ppm): 7.64 (1H, d, J = 4.0 Hz), 7.40 (1H, d, J = 4.0 Hz), 4.80 (1H, s).

*Step 4: 5-Ethynylthiophene-2-carboxylic Acid Tetrahydropyran-2-yloxyamide (**15**).* To a solution of **14** (150 mg, 0.986 mmol), EDCI (226 mg, 1.18 mmol), and HOBt·H_2O (159 mg, 1.18 mmol) in DMF (3 mL) was added NH_2OTHP (173 mg, 1.48 mmol), and the mixture was stirred at room temperature for 24 h. The reaction mixture was poured into water and extracted with AcOEt. The organic layer was separated, washed with saturated $NaHCO_3$ and brine, and dried over Na_2SO_4. Filtration, concentration in vacuo, and purification of the residue by silica gel flash column chromatography (AcOEt/*n*-hexane = 1/30) gave 224 mg (90%) of **15** as a yellow solid. ^{1}H NMR (DMSO-d_6, 500 MHz, δ; ppm): 11.9 (1H, broad s), 7.62 (1H, d, J = 4.0 Hz), 7.39 (1H, d, J = 4.0 Hz), 4.96 (1H, s), 4.77 (1H, s), 4.05–4.01 (1H, m), 3.55–3.53 (1H, m), 1.73–1.71 (3H, m), 1.55–1.53 (3H, m).

*Step 5: Preparation of 5-Ethynylthiophene-2-carboxylic Acid Hydroxyamide (**A2**).* To a solution of **15** (224 mg, 0.891 mmol) obtained above in MeOH (10 mL) was added TsOH·H_2O (16.9 mg, 0.0891 mmol). The reaction mixture was stirred for 12 h at room temperature. After removal of the solvent, the residue was purified by silica gel flash column chromatography (AcOEt/*n*-hexane = 1/1) to give 147 mg (77%) of **A2** as a brown solid; mp 146–147 °C. ^{1}H NMR (DMSO-d_6, 500 MHz, δ; ppm): 11.4 (1H, broad s), 9.25 (1H, broad s), 7.53 (1H, d, J = 4.0 Hz), 7.36 (1H, d, J = 4.0 Hz), 4.74 (1H, s). ^{13}C NMR ($CDCl_3$, 125 MHz, δ; ppm): 158.32, 138.73, 133.83, 127.36, 124.66, 86.93, 76.20. MS (EI) m/z 167 (M^+); Anal. Calcd for $C_7H_5NO_2S$·1/5H_2O: C, 49.23; H, 3.19; N, 8.20. Found: C, 49.10; H, 3.18; N, 8.07.

Compounds **A3** and **A4** were prepared from **16a** and **16b**, respectively, using the same procedure described for **A2**.

*3-Ethynyl-N-hydroxybenzamide (**A3**).* Yield 68%; colorless crystals; mp 165–166 °C. ^{1}H NMR (DMSO-d_6, 500 MHz, δ; ppm): 11.3 (1H, broad s), 9.14 (1H, broad s), 7.82 (1H, s), 7.78 (1H, d, J = 7.9 Hz), 7.62 (1H, d, J = 7.6 Hz), 7.49 (1H, t, J = 7.8 Hz), 4.28 (1H, s). ^{13}C NMR (DMSO-d_6, 150 MHz, δ; ppm): 163.07, 134.07, 133.08, 129.81, 128.89, 127.35, 121.75, 82.65, 81.40. MS (EI) m/z: 161 (M^+). Anal. ($C_9H_7NO_2$) C, H, N.

*4-Ethynyl-N-hydroxybenzamide (**A4**).* Yield 47%; colorless crystals; mp 166–167 °C. ^{1}H NMR (DMSO-d_6, 500 MHz, δ; ppm): 11.3 (1H, broad s), 9.12 (1H, broad s), 7.75 (2H, d, J = 8.2 Hz), 7.55 (2H, d, J = 8.2 Hz), 4.37 (1H, s). ^{13}C NMR (DMSO-d_6, 150 MHz, δ; ppm): 163.24, 132.77, 131.61, 127.04, 124.25, 82.72, 82.66. MS (EI) m/z 161 (M^+). Anal. ($C_9H_7NO_2$·1/10H_2O) C, H, N.

*Propynoic Acid 2-Aminophenylamide (**A5**).* Compound **A5** was prepared as colorless crystals in 44% yield from **8** and 1,2-phenylenediamine, using the same procedure described for **A1** (step 1); mp 127–128 °C. ^{1}H NMR (DMSO-d_6, 500 MHz, δ; ppm): 9.97 (1H, s), 7.15 (1H, d, J = 7.9 Hz), 6.93 (1H, t, J = 7.6 Hz), 6.73 (1H, d, J = 7.9 Hz), 6.55 (1H, t, J = 7.6 Hz), 4.91 (2H, s), 4.32 (1H, s). ^{13}C NMR (DMSO-d_6, 125 MHz, δ; ppm): 149.94, 141.94, 126.59, 125.52, 121.65, 116.01, 115.96, 78.43, 76.61. MS (EI) m/z 160 (M^+). Anal. ($C_9H_8N_2O$) C, H, N.

Compounds **A6–A8** were prepared from 1,2-phenylenediamine and the corresponding carboxylic acids **14** and **189a,b** using the same procedure described for **A2** (step 4).

*5-Ethynylthiophene-2-carboxylic Acid 2-Aminophenylamide (**A6**).* Yield 79%; colorless crystals; mp 143 °C. ^{1}H NMR (DMSO-d_6, 500 MHz, δ; ppm): 9.88 (1H, broad s), 7.98 (1H, d, J = 4.0 Hz), 7.51 (1H, d, J = 4.0 Hz), 7.17 (1H, d, J = 7.9 Hz), 7.07–7.04 (1H, m), 6.86–6.84 (1H, m), 6.68–6.64 (1H, m), 5.01 (2H, s), 4.83 (1H, s). ^{13}C NMR ($CDCl_3$, 125 MHz, δ; ppm): 159.04, 143.46, 141.22, 133.93, 128.97, 127.03, 126.98, 125.45, 122.13, 116.17, 116.01, 87.04, 76.42. MS (EI) m/z 242 (M^+). Anal. ($C_7H_5NO_2S$·1/4H_2O) C, H, N.

*N-2-Aminophenyl-3-ethynylbenzamide (**A7**).* Yield 91%; colorless crystals; mp 194–195 °C. ^{1}H NMR (DMSO-d_6, 500 MHz, δ; ppm): 9.73 (1H, broad s), 8.09 (1H, broad s), 7.99 (1H, d, J = 7.9 Hz), 7.67 (1H, d, J = 7.6 Hz), 7.53 (1H, t, J = 7.8 Hz), 7.15 (1H, d, J = 7.9 Hz), 6.97 (1H, m), 6.78 (1H, dd, J = 1.2, 7.9 Hz), 6.59 (1H, t, J = 7.3 Hz), 4.93 (2H, broad s), 4.30 (1H, s). ^{13}C NMR (DMSO-d_6, 150 MHz, δ; ppm): 164.47, 143.28, 135.09, 134.35, 130.88, 128.85, 128.38, 126.86, 126.69, 122.96, 121.76, 116.20, 116.06, 82.92, 81.43. MS (EI) m/z: 236 (M^+). Anal. ($C_{15}H_{12}N_2O$·1/3H_2O) C, H, N.

*N-2-Aminophenyl-4-ethynylbenzamide (**A8**).* Yield 86%; colorless crystals; mp 181–183 °C. ^{1}H NMR (DMSO-d_6, 500 MHz, δ; ppm): 9.73 (1H, broad s), 7.99 (2H, d, J = 7.9 Hz), 7.61 (2H, d, J = 8.5 Hz), 7.15 (1H, d, J = 7.3 Hz), 6.99–6.96 (1H, m), 6.78–6.77 (1H, m), 6.61–6.58 (1H, m), 4.92 (2H, s), 4.41 (1H, s). ^{13}C NMR (DMSO-d_6, 125 MHz, δ; ppm): 164.41, 143.13, 134.62, 131.47, 127.96, 126.67, 126.52, 124.45, 122.90, 116.06, 115.95, 82.82, 82.79. MS (EI) m/z 236 (M^+). Anal. ($C_{15}H_{12}$N2O·1/5H_2O) C, H, N.

General Procedure for the Synthesis of Azides B2–B9, B11, B12, B14, B16–B34, B36, and B45. To a 0.5 M solution of NaN_3 (1.1 equiv) in DMSO was added an appropriate alkyl halide (1.0 equiv), and the mixture was stirred at room temperature or 80 °C and periodically monitored by TLC. When the reaction was completed, the mixture was quenched with water and stirred until it cooled to room temperature and then extracted with AcOEt or Et_2O. The organic layer was separated, washed with water and brine, and dried over Na_2SO_4. Filtration, concentration in vacuo, and purification of the residue by silica gel flash column chromatography gave the corresponding alkyl azide.

*Phenethyl Azide (**B2**).*[26] Yield 76%; a pale-yellow oil. ^{1}H NMR ($CDCl_3$, 500 MHz, δ; ppm): 7.33–7.21 (5H, m), 3.50 (2H, t, J = 7.3 Hz), 2.89 (2H, t, J = 7.31 Hz). ^{13}C NMR ($CDCl_3$, 150 MHz, δ; ppm): 137.99, 128.72, 128.62, 126.76, 52.44, 35.33. FTIR (neat, cm^{-1}) 2090. MS (EI) m/z 119 (M^+ − 28).

*3-Phenylpropyl Azide (**B3**).*[26] Yield 55%; a pale-yellow oil. ^{1}H NMR ($CDCl_3$, 500 MHz, δ; ppm): 7.31–7.17 (5H, m), 3.28 (2H, t, J = 6.9 Hz), 2.69 (2H, t, J = 7.6 Hz), 1.91 (2H, m). ^{13}C NMR ($CDCl_3$, 150 MHz, δ; ppm): 140.85, 128.51, 128.45, 126.14,50.64, 32.76, 30.43. FTIR (neat, cm^{-1}) 2090. MS (EI) m/z 133 (M^+ − 28).

*4-Phenylbutyl Azide (**B4**).*[27] Yield 58%; a pale-yellow oil. ^{1}H NMR ($CDCl_3$, 500 MHz, δ; ppm): 7.30–7.17 (5H, m), 3.28 (2H, t, J = 6.9 Hz), 2.65 (2H, t, J = 7.5 Hz), 1.74–1.68 (2H, m), 1.66–1.60 (2H, m). ^{13}C NMR ($CDCl_3$, 125 MHz, δ; ppm): 141.80, 128.37, 128,35, 125.89, 51.34, 35.35, 28.42. FTIR (neat, cm^{-1}) 2090.

*5-Phenylpentyl Azide (**B5**).* Yield 75%; a pale-yellow oil. ^{1}H NMR ($CDCl_3$, 500 MHz, δ; ppm): 7.29–7.16 (5H, m), 3.25 (2H, t, J = 7.0 Hz), 2.65 (2H, t, J = 7.6 Hz), 1.68–1.59 (4H, m), 1.44–1.38 (2H, m). ^{13}C NMR ($CDCl_3$, 125 MHz, δ; ppm): 142.26, 128.34, 128.29, 125.73, 51.34, 35.74, 30.94, 28.72, 26.34. FTIR (neat, cm^{-1}) 2090. MS (EI) m/z 133 (M^+ − 28).

*4-Methoxybenzyl Azide (**B6**).*[28] Yield 60%; a pale-yellow oil. ^{1}H NMR ($CDCl_3$, 500 MHz, δ; ppm): 7.24 (2H, d, J = 8.8 Hz), 6.91 (2H, d, J = 8.5 Hz), 4.26 (2H, s), 3.81(2H, s). ^{13}C NMR ($CDCl_3$, 150 MHz, δ; ppm): 159.60, 129.72, 127.36, 114.16, 55.26, 54.36. FTIR (neat, cm^{-1}) 2090. MS (EI) m/z 163 (M^+). HRMS (EI) calcd for $C_8H_9ON_3$, 163.0758; found, 163.0761.

*3-Phenylbenzyl Azide (**B7**).* Yield 78%; colorless crystals. ^{1}H NMR ($CDCl_3$, 500 MHz, δ; ppm): 7.59−7.52 (4H, m), 7.37−7.34 (1H, m), 7.46−7.42 (3H, m), 7.29 (1H, d, J = 7.6 Hz), 4.39 (2H, s). ^{13}C NMR ($CDCl_3$, 125 MHz, δ; ppm): 141.95, 140.66, 135.94, 129.28, 128.84, 127.56, 127.20, 127.14, 127.00, 126.98, 54.87. FTIR (neat, cm^{-1}) 2094. MS (EI) m/z 209 (M^+). HRMS (EI) calcd for $C_{13}H_{11}N_3$, 209.0957; found, 209.0960.

*4-Phenylbenzyl Azide (**B8**).* Yield 21%; a pale-yellow oil. ^{1}H NMR ($CDCl_3$, 500 MHz, δ; ppm): 7.62−7.59 (4H, m), 7.45 (2H, t, J = 7.6 Hz), 7.40−7.35 (3H, m), 4.39 (2H, s). ^{13}C NMR ($CDCl_3$, 125 MHz, δ; ppm): 141.31, 140.54, 134.37, 128.84, 128.67, 127.58, 127.52, 127.13, 54.57. FTIR (neat, cm^{-1}) 2090. MS (EI) m/z 209 (M^+). HRMS (EI) calcd for $C_{13}H_{11}N_3$, 209.0952; found, 209.0953.

*3-Phenoxybenzyl Azide (**B9**).* Yield 86%; a pale-yellow oil. ^{1}H NMR ($CDCl_3$, 500 MHz, δ; ppm): 7.37−7.32 (3H, m), 7.12 (1H, t, J = 7.5 Hz), 7.05−7.01 (3H, m), 6.96−6.89 (2H, m), 4.30 (2H, s). ^{13}C NMR ($CDCl_3$, 125 MHz, δ; ppm): 157.79, 156.78, 137.29, 130.19, 129.85, 123,60, 122.77, 119.15, 118.48, 118.27, 54.42. FTIR (neat, cm^{-1}) 2090. MS (EI) m/z 225 (M^+). HRMS calcd for $C_{13}H_{11}ON_3$, 225.0901; found, 225.0902.

*1-Azidomethylnaphthalene (**B11**).* Yield 91%; a pale-yellow oil. ^{1}H NMR ($CDCl_3$, 500 MHz, δ; ppm): 8.01 (1H, d, J = 8.2 Hz), 7.88−7.83 (2H,m), 7.58− 7.50 (2H, m), 7.46−7.42 (2H, m), 4.74 (2H, s). ^{13}C NMR ($CDCl_3$, 125 MHz, δ; ppm): 133.87, 131.32, 130.93, 129.39, 128.77, 127.23, 126.69, 126.12, 125.17, 123.442, 52.97. FTIR (neat, cm^{-1}) 2094. MS (EI) m/z 183 (M^+). HRMS (EI) calcd for $C_{11}H_9N_3$, 183.0804; found, 183.0802.

*2-Azidomethylnaphthalene (**B12**).*[29] Yield 83%; colorless crystals. ^{1}H NMR ($CDCl_3$, 500 MHz, δ; ppm): 7.88−7.84 (3H, m), 7.78 (1H, s), 7.53−7.49 (2H, m), 7.43 (1H, dd, J = 1.5, 8.2 Hz), 4.51 (2H, s). ^{13}C NMR ($CDCl_3$, 125 MHz, δ; ppm): 133.28, 133.11, 132.83, 128.79, 127.96, 127.77, 127.19, 126.48, 126.35, 125,86, 55.05. FTIR (neat, cm^{-1}) 2090. MS (EI) m/z 183 (M^+). HRMS (EI) calcd for $C_{11}H_9N_3$, 183.0803; found. 183.0803.

*Azidomethylcyclohexane (**B14**).* Yield 92%; a pale-yellow oil. ^{1}H NMR ($CDCl_3$, 500 MHz, δ; ppm): 3.11 (2H, d, J = 6.7 Hz), 1.78−1.67 (5H, m), 1.59−1.51 (1H, m), 1.29−1.11 (3H, m), 1.01−0.92 (2H, m). ^{13}C NMR ($CDCl_3$, 125 MHz, δ; ppm): 58.08, 38.09, 30.67, 26.27, 25.76. FTIR (neat, cm^{-1}) 2094.

*2-Methylphenethyl Azide (**B16**).* Yield 95%; a colorless oil. ^{1}H NMR ($CDCl_3$, 500 MHz, δ; ppm): 7.16 (4H, s), 3.47 (2H, t, J = 7.6 Hz), 2.91 (2H, t, J = 7.6 Hz), 2.34 (3H, s). ^{13}C NMR ($CDCl_3$, 125 MHz, δ; ppm): 136.20, 136.07, 130.48, 129.34, 126.96, 126.25, 51.44, 32.62, 19.31. FTIR (neat, cm^{-1}) 2090. MS (EI) m/z 133 (M^+ − 28).

*3-Methylphenethyl Azide (**B17**).* Yield 81%; a colorless oil. ^{1}H NMR ($CDCl_3$, 500 MHz, δ; ppm): 7.21 (1H, t, J = 7.5 Hz), 7.07−7.01 (3H, m), 3.49 (2H, t, J = 7.3 Hz), 2.86 (2H, t, J = 7.3 Hz), 2.34 (3H, s). ^{13}C NMR ($CDCl_3$, 125 MHz, δ; ppm): 138.28, 137.94, 129.55, 128.54, 127.52, 125.73, 52.50, 35.27, 21.38. FTIR (neat, cm^{-1}) 2090. MS (EI) m/z 133 (M^+ − 28).

*4-Methylphenethyl Azide (**B18**).* Yield 85%; a colorless oil. ^{1}H NMR ($CDCl_3$, 500 MHz, δ; ppm): 7.13 (2H, d, J = 8.2 Hz), 7.11 (2H, d, J = 8.2 Hz), 3.48 (2H, t, J = 7.3 Hz), 2.86 (2H, t, J = 7.3 Hz), 2.33 (3H, s). ^{13}C NMR ($CDCl_3$, 125 MHz, δ; ppm): 136.36, 134.92, 129.33, 128.62, 52.59, 34.92, 21.05. FTIR (neat, cm^{-1}) 2090;. HRMS (EI) calcd for $C_9H_{11}N_3$, 161.0950; found, 161.0947.

*2-Methoxyphenethyl Azide (**B19**).* Yield 72%; a pale-yellow oil. ^{1}H NMR ($CDCl_3$, 500 MHz, δ; ppm): 7.24 (1H, dt, J = 1.8, 5.9 Hz), 7.16 (2H, dd, J = 1.5, 5.8 Hz), 6.91 (1H, dt, J = 1.2, 6.2 Hz), 6.86 (1H, d, J = 8.2 Hz), 3.83 (3H, s), 3.47 (2H, t, J = 7.6 Hz), 2.92 (2H, t, J = 7.6 Hz). ^{13}C NMR ($CDCl_3$, 125 MHz, δ; ppm): 157.57, 130.61, 128.17, 126.23, 120.56, 110.35, 55.24, 50.97, 30.34. FTIR (neat, cm^{-1}) 2090. HRMS (EI) calcd for $C_9H_{11}ON_3$, 177.0901; found, 177.0903.

*3-Methoxyphenethyl Azide (**B20**).* Yield 89%; a colorless oil. ^{1}H NMR ($CDCl_3$, 500 MHz, δ; ppm): 7.24 (1H, t, J = 7.9 Hz), 6.82−6.76 (3H, m), 3.81 (3H, s), 3.50 (2H, t, J = 7.3 Hz), 2.87 (2H, t, J = 7.3 Hz). ^{13}C NMR ($CDCl_3$, 125 MHz, δ; ppm): 159.83, 139.61, 129.66, 121.07, 114.62, 112.05, 55.20, 52.38, 35.40. FTIR (neat, cm^{-1}) 2090. HRMS (EI) calcd for $C_9H_{11}ON_3$, 177.0909; found, 177.0910.

*4-Methoxyphenethyl Azide (**B21**).* Yield 100%; a pale-yellow oil. ^{1}H NMR ($CDCl_3$, 500 MHz, δ; ppm): 7.14 (2H, d, J = 8.8 Hz), 6.86 (2H, d, J = 8.5 Hz), 3.80 (3H, s), 3.46 (2H, t, J = 7.2 Hz), 2.84 (2H, t, J = 7.2 Hz). ^{13}C NMR ($CDCl_3$, 125 MHz, δ; ppm): 158.50, 130.06, 129.73, 114.09, 55.28, 52.73, 34.50. FTIR (neat, cm^{-1}) 2090. HRMS (EI) calcd for $C_9H_{11}ON_3$, 177.0904; found, 177.0903.

*2-Chlorophenethyl Azide (**B22**).* Yield 90%; a colorless oil. ^{1}H NMR ($CDCl_3$, 500 MHz, δ; ppm): 7.37 (1H, d, J = 7.0 Hz), 7.26−7.21 (3H, m), 3.53 (2H, t, J = 7.3 Hz), 3.03 (2H, t, J = 7.3 Hz). ^{13}C NMR ($CDCl_3$, 125 MHz, δ; ppm): 135.57, 134.07, 131.11, 129.71, 128.39, 127.02, 50.63, 33.29. FTIR (neat, cm^{-1}) 2090. HRMS (EI) calcd for $C_8H_8N_3Cl$, 181.0405; found, 181.0404.

*3-Chlorophenethyl Azide (**B23**).* Yield 80%; a pale-yellow oil. ^{1}H NMR ($CDCl_3$, 500 MHz, δ; ppm): 7.25−7.22 (3H, m), 7.11 (1H, d, J = 6.7 Hz), 3.51 (2H, t, J = 7.2 Hz), 2.87 (2H, t, J = 7.2 Hz). ^{13}C NMR ($CDCl_3$, 125 MHz, δ; ppm): 140.06, 134.43, 129.90, 128.92, 127.04, 126.97, 52.13, 35.03. FTIR (neat, cm^{-1}) 2090. MS (EI) m/z 153 (M^+ − 28).

*4-Chlorophenethyl Azide (**B24**).* Yield 92%; a colorless oil. ^{1}H NMR ($CDCl_3$, 500 MHz, δ; ppm): 7.29 (2H, d, J = 8.2 Hz), 7.15 (2H, d, J = 8.2 Hz), 3.49 (2H, t, J = 7.2 Hz), 2.86 (2H, t, J = 7.2 Hz). ^{13}C NMR ($CDCl_3$, 125 MHz, δ; ppm): 136.52, 132.66, 130.11, 128.79, 52.27, 34.72. FTIR (neat, cm^{-1}) 2090. HRMS (EI) calcd for $C_8H_8N_3Cl$, 181.0406; found, 181.0404.

*2-Fluorophenethyl Azide (**B25**).* Yield 82%; a colorless oil. ^{1}H NMR ($CDCl_3$, 500 MHz, δ; ppm): 7.26−7.22 (2H, m), 7.11−7.03 (2H, m), 3.52 (2H, t, J = 7.0 Hz), 2.94 (2H, t, J = 7.0 Hz). ^{13}C NMR ($CDCl_3$, 150 MHz, δ; ppm): 161.24, 131.15, 128.69, 124.90, 124.23, 115.45, 51.08, 29.00. FTIR (neat, cm^{-1}) 2090. MS (EI) m/z 137 (M^+ − 28).

*3-Fluorophenethyl Azide (**B26**).* Yield 95%; a colorless oil. ^{1}H NMR ($CDCl_3$, 500 MHz, δ; ppm): 7.31−7.26 (1H, m), 7.01−6.93 (3H, m), 3.52 (2H, t, J = 7.3 Hz), 2.89 (2H, t, J = 7.3 Hz). ^{13}C NMR ($CDCl_3$, 125 MHz, δ; ppm): 162.96, 140.54, 130.12, 124.42, 115.69, 113.75, 52.13, 35.09. FTIR (neat, cm^{-1}) 2090. MS (EI) m/z 137 (M^+ − 28).

*4-Fluorophenethyl Azide (**B27**).* Yield 95%; a colorless oil. ^{1}H NMR ($CDCl_3$, 500 MHz, δ; ppm): 7.19−7.17 (2H, m), 7.01 (2H, t, J = 8.7 Hz), 3.49 (2H, t, J = 7.3 Hz), 2.86 (2H, t, J = 7.3 Hz). ^{13}C NMR ($CDCl_3$, 125 MHz, δ; ppm): 161.83, 133.72, 130.22, 115.49, 52.51, 34.58. FTIR (neat, cm^{-1}) 2090. HRMS (EI) calcd for $C_8H_8N_3Cl$, 165.0702; found, 165.0701.

*2-(Trifluoromethyl)phenethyl Azide (**B28**).* Yield 88%; a colorless oil. ^{1}H NMR ($CDCl_3$, 500 MHz, δ; ppm): 7.66 (1H, d, J = 7.6 Hz), 7.51 (1H, t, J = 7.6 Hz), 7.39− 7.35 (2H, m), 3.51 (2H, t, J = 7.3 Hz), 3.08 (2H, t, J = 7.3 Hz). ^{13}C NMR ($CDCl_3$, 125 MHz, δ; ppm): 131.93, 131.73, 128.99, 127.00, 126.29, 125.56, 123.38, 52.08, 32.30. FTIR (neat, cm^{-1}) 2094. MS (EI) m/z 187 (M^+ − 28).

*3-(Trifluoromethyl)phenethyl Azide (**B29**).* Yield 87%; a colorless oil. ^{1}H NMR ($CDCl_3$, 600 MHz, δ; ppm): 7.52 (1H, d, J = 7.8 Hz), 7.48 (1H, s), 7.46− 7.41 (2H, m). ^{13}C NMR ($CDCl_3$, 125 MHz, δ; ppm): 139.01, 132.22, 129.11, 125.52, 123.74, 52.11, 35.16. FTIR (neat, cm^{-1}) 2094. MS (EI) m/z 153 (M^+ − 28).

*4-(Trifluoromethyl)phenethyl Azide (**B30**).* Yield 90%; a pale-yellow oil. ^{1}H NMR ($CDCl_3$, 600 MHz, δ; ppm): 7.58 (2H, d, J = 8.1 Hz), 7.34 (2H, d, J = 8.0 Hz), 3.55 (2H, t, J = 7.1 Hz), 2.95 (2H, t, J = 7.1 Hz). ^{13}C NMR ($CDCl_3$, 150 MHz, δ; ppm): 142.16, 129.13, 125.60, 125.08, 123.27, 52.02, 35.16. FTIR (neat, cm^{-1}) 2094. MS (EI) m/z 153 (M^+ − 28).

*2-Nitrophenethyl Azide (**B31**).* Yield 91%; a yellow oil. ^{1}H NMR ($CDCl_3$, 500 MHz, δ; ppm): 7.99 (1H, d, J = 8.2 Hz), 7.58 (1H, t, J = 7.5 Hz), 7.45−7.41 (2H, m), 3.64 (2H, t, J = 6.9 Hz), 3.18 (2H, t, J = 6.9 Hz). ^{13}C NMR ($CDCl_3$, 125 MHz, δ; ppm): 149.34, 133.28, 133.13, 132.86, 128.14, 125.14, 51.48, 33.00. FTIR (neat, cm^{-1}) 2090, 1519, 1342. MS (EI) m/z 164 (M^+ − 28).

*3-Nitrophenethyl Azide (**B32**).* Yield 62%; a yellow oil. ^{1}H NMR ($CDCl_3$, 500 MHz, δ; ppm): 8.13−8.11 (2H, m), 7.58 (1H, d J = 7.6 Hz), 7.51 (1H, t J = 7.8 Hz), 3.60 (2H, t, J = 6.9 Hz), 3.00 (2H, t, J = 6.9 Hz). ^{13}C NMR ($CDCl_3$, 125 MHz, δ; ppm): 148.47, 140.15,

135.09, 129.58, 123.70, 122.01, 51.86, 34.98. FTIR (neat, cm^{-1}) 2090, 1523, 1346. MS (EI) m/z 164 ($M^+ - 28$).

*4-Nitrophenethyl Azide (**B33**).* Yield 93%; a yellow oil. ^1H NMR ($CDCl_3$, 500 MHz, δ; ppm): 8.19 (2H, d, J = 8.5 Hz), 7.40 (2H, d, J = 8.5 Hz), 3.59 (2H, t, J = 6.9 Hz), 3.00 (2H, t, J = 6.9 Hz). ^{13}C NMR ($CDCl_3$, 125 MHz, δ; ppm): 147.05, 145.77, 129.70, 123.89, 51.72, 35.19. FTIR (neat, cm^{-1}) 2090, 1516, 1342. MS (EI) m/z 164 ($M^+ - 28$).

*1-(2-Azidoethyl)naphthalene (**B34**).* Yield 91%; a yellow oil. ^1H NMR ($CDCl_3$, 500 MHz, δ; ppm): 8.00 (1H, d, J = 8.5 Hz), 7.89−7.87 (1H, m), 7.77 (1H, d, J = 8.2 Hz), 7.56−7.38 (4H, m), 3.64 (2H, t, J = 7.6 Hz), 3.38 (2H, t, J = 7.6 Hz). ^{13}C NMR ($CDCl_3$, 150 MHz, δ; ppm): 133.93, 133.86, 131.70, 129.01, 127.68, 127.00, 126.27, 125.72, 125.55, 123.14, 51.74, 32.49. FTIR (neat, cm^{-1}) 2090. HRMS (EI) calcd for $C_{12}H_{11}N_3$, 197.0953; found, 197.0954.

*3-(2-Azidoethyl)indole (**B36**).* Yield 92%; a pale-yellow oil. ^1H NMR ($CDCl_3$, 500 MHz, δ; ppm): 8.01 (1H, s), 7.59 (1H, dd, J = 1.2, 7.9 Hz), 7.37 (1H, dt, J = 0.9, 8.2 Hz), 7.21 (1H, m), 7.14 (1H, m), 7.07 (1H, d, J = 2.4 Hz), 3.57 (2H, t, J = 7.2 Hz), 3.07 (2H, dt, J = 0.9, 7.0 Hz). ^{13}C NMR ($CDCl_3$, 150 MHz, δ; ppm): 136.25, 127.13, 122.24, 122.21, 119.56, 118.52, 112.37, 111.27, 51.66, 25.09. FTIR (neat, cm^{-1}) 2090. HRMS (EI) calcd for $C_{10}H_{10}N_4$, 186.0906; found, 186.0904.

*2-Azidoacetophenone (**B45**).* Yield 53%; a yellow oil. ^1H NMR ($CDCl_3$, 500 MHz, δ; ppm): 7.93−7.90 (2H, m), 7.65−7.61 (1H, m), 7.52−7.49 (2H, m), 4.57 (2H, s). ^{13}C NMR ($CDCl_3$, 150 MHz, δ; ppm): 193.19, 134.41, 134.15, 129.00, 127.95, 54.90. FTIR (neat, cm^{-1}) 2098, 1693. MS (EI) m/z 133 ($M^+ - 28$).

*Azidomethylcyclopentane (**B13**). Step 1: Preparation of Cyclopentylmethyl Tosylate (**23a**).* To a solution of cyclopentanemethanol (**22a**, 500 mg, 4.99 mmol) in pyridine (5 mL) was added TsCl (1.43 g, 7.49 mmol) at 0 °C. The reaction mixture was stirred for 36 h at room temperature. After removal of the solvent, the residue was diluted with AcOEt. The AcOEt solution was washed with saturated $NaHCO_3$ and brine and dried over Na_2SO_4. Filtration, concentration in vacuo, and purification of the residue by silica gel flash column chromatography (AcOEt/*n*-hexane = 1/50) gave 864 mg (68%) of **23a** as a colorless oil. ^1H NMR ($CDCl_3$, 500 MHz, δ; ppm): 7.79 (2H, d, J = 8.2 Hz), 7.35 (2H, d, J = 7.9 Hz), 3.89 (2H, d, J = 7.3 Hz), 2.50 (3H, s), 2.24−2.15 (1H, m), 1.74−1.68 (2H, m), 1.57−1.49 (4H, m), 1.22−1.15 (2H, m).

*Step 2: Preparation of Azidomethylcyclopentane (**B13**).* To a 0.5 M solution of NaN_3 in DMSO (26.6 mL, 13.3 mmmol) was added **23a** (1.13 g, 13.3 mmmol) obtained above, and the mixture was stirred at 80 °C for 5 h. The reaction mixture was quenched with water and stirred until it cooled to room temperature, then extracted with AcOEt. The AcOEt layer was separated, washed with water and brine, and dried over Na_2SO_4. Filtration and concentration in vacuo gave 147 mg (26%) of **B13** as a yellow oil. ^1H NMR ($CDCl_3$, 500 MHz, δ; ppm): 3.20 (2H, d, J = 7.3 Hz), 2.19−2.10 (1H, m), 1.83−1.77 (2H, m), 1.64−1.55 (4H, m), 1.29−1.21 (2H, m). ^{13}C NMR ($CDCl_3$, 125 MHz, δ; ppm): 56.51, 39.64, 30.33, 25.28; FTIR (neat, cm^{-1}) 2098.

Azides **B15** and **B41**−**B43** were prepared from the corresponding alcohols using the same procedure described for **B13**.

*1-Azidomethyladamantane (**B15**).*[30] Yield 45%; a colorless oil. ^1H NMR ($CDCl_3$, 500 MHz, δ; ppm): 2.95 (2H, s), 1.99 (3H, s), 1.72 (3H, d, J = 12 Hz), 1.64 (3H, d, J = 12 Hz), 1.52 (6H, d, J = 2.4 Hz). ^{13}C NMR ($CDCl_3$, 125 MHz, δ; ppm): 64.37, 40.09, 36.85, 34.78, 28.21. FTIR (neat, cm^{-1}) 2094. MS (EI) m/z 191 (M^+). HRMS (EI) calcd for $C_{11}H_{17}N_3$, 191.1423; found, 191.1424.

*(2-Azidoethyl)cyclopentane (**B41**).* Yield 53%; a pale-yellow oil. ^1H NMR ($CDCl_3$, 500 MHz, δ; ppm): 3.27 (2H, t, J = 7.3 Hz), 1.87−1.78 (3H, m), 1.64−1.62 (4H, m), 1.60−1.49 (2H, m). ^{13}C NMR ($CDCl_3$, 150 MHz, δ; ppm): 50.83, 37.41, 34.92, 32.48, 25.05. FTIR (neat, cm^{-1}) 2090.

*(2-Azidoethyl)cyclohexane (**B42**).* Yield 55%; a pale-yellow oil. ^1H NMR ($CDCl_3$, 500 MHz, δ; ppm): 3.29 (2H, t, J = 7.2 Hz), 1.72−1.61 (5H, m), 1.50 (2H, q, J = 7.1 Hz), 1.38−1.37 (1H, m), 1.28−1.11 (3H, m), 0.951 (2H, m). ^{13}C NMR ($CDCl_3$, 125 MHz, δ; ppm): 49.20, 36.05, 35.00, 33.02, 26.44, 26.14. FTIR (neat, cm^{-1}) 2090.

*(2-Azidoethyl)-1-adamantane (**B43**).* Yield 79%; a colorless oil. ^1H NMR ($CDCl_3$, 500 MHz, δ; ppm): 3.27 (2H, t, J = 7.9 Hz), 1.96 (3H, s), 1.72−1.62 (6H, m), 1.51 (6H, d, J = 2.1 Hz), 1.40 (2H, t, J = 7.9 Hz). ^{13}C NMR ($CDCl_3$, 125 MHz, δ; ppm): 46.61, 42.42, 42.34, 36.98, 31.80, 30.93, 28.55. FTIR (neat, cm^{-1}) 2090.

*4-Phenoxybenzyl Azide (**B10**). Step 1: 4-Phenoxyphenylmethanol (**25**).* A solution of 4-phenoxybenzoic acid (**24**, 2.00 g, 9.34 mmol) in THF (45 mL) was added dropwise to a suspension of $LiAlH_4$ (1.06 g, 28.0 mmol) in THF (65.0 mL) with cooling by an ice-bath. The mixture was heated at reflux for 7 h. After cooling of the reaction mixture, water (1.00 mL), 15% aqueous NaOH (1.00 mL), and water (3.00 mL) were successively added, and the slurry was filtered. The solid was washed with THF, the combined filtrates were concentrated in vacuo, and the residue was purified by silica gel flash column chromatography (AcOEt/*n*-hexane = 1/3) to give 1.63 g (87%) of **25** as a white solid. ^1H NMR ($CDCl_3$, 500 MHz, δ; ppm): 7.35−7.31 (4H, m), 7.10 (1H, t, J = 7.5 Hz), 7.02−7.00 (4H, m), 4.67 (2H, d, J = 5.8 Hz).

*Step 2: Preparation of 4-Phenoxybenzyl Azide (**B10**).* To a mixture of **25** (300 mg, 1.50 mmol) obtained above and DPPA (495 mg, 1.80 mmol) in dry DMF (2.7 mL) was added neat DBU (274 mg, 1.80 mmol) at 0 °C under Ar. The reaction mixture was stirred at room temperature for 24 h and then poured into water and extracted with AcOEt. The AcOEt layer was separated, washed with water, 2 N aqueous HCl, and brine, and dried over Na_2SO_4. Filtration, concentration in vacuo, and purification of the residue by silica gel flash column chromatography (AcOEt/*n*-hexane = 1/50) gave 103 mg (30%) of **B10** as a colorless oil. ^1H NMR ($CDCl_3$, 500 MHz, δ; ppm): 7.37−7.31 (2H, m), 7.10 (1H, t, J = 7.5 Hz), 7.02−7.00 (4H, m), 2H (d, J = 5.8 Hz). ^{13}C NMR ($CDCl_3$, 125 MHz, δ; ppm): 157.49, 156.81, 130.01, 129.81, 123.57, 119.15, 118.89, 54.30. FTIR (neat, cm^{-1}) 2090. MS (EI) m/z 225 (M^+). HRMS (EI) calcd for $C_{13}H_{11}ON_3$, 225.0903; found, 225.0900.

*2-(2-Azidoethyl)naphthalene (**B35**).* To a solution of 2-naphthaleneethanol (**27a**, 1.00 g, 5.81 mmol) in CH_2Cl_2 (4 mL) were added triethylamine (705 mg, 6.97 mmol) and MsCl (798 mg, 6.97 mmol) at 0 °C. The mixture was stirred for 3 h at room temperature and then poured into saturated aqueous $NaHCO_3$ and extracted with $CHCl_3$. The organic layer was washed with water and brine and dried over Na_2SO_4. Filtration and concentration in vacuo gave the crude mesylate. To a 0.5 M solution of NaN_3 in DMSO (13.9 mL, 6.97 mmmol) was added the mesylate, and the mixture was stirred at 80 °C for 2 h and then poured into water and extracted with AcOEt. The AcOEt layer was washed with water and brine and dried over Na_2SO_4. Filtration, concentration in vacuo, and purification of the residue by silica gel flash column chromatography (AcOEt/*n*-hexane = 1/50) gave 906 mg (79%, 2 steps) of **B35** as a white solid. The solid was recrystallized from AcOEt/*n*-hexane to give 319 mg of **B35** as a white solid. ^1H NMR ($CDCl_3$, 500 MHz, δ; ppm): 7.83−7.79 (3H, m), 7.68 (1H, s), 7.49−7.43 (2H, m), 7.35 (1H, dd, J = 1.8, 8.2 Hz), 3.60 (2H, t, J = 7.3 Hz), 3.06 (2H, t, J = 7.3 Hz). ^{13}C NMR ($CDCl_3$, 125 MHz, δ; ppm): 135.49, 133.58, 132.38, 128.33, 127.69, 127.55, 127.31, 126.98, 126.19, 125.65, 52.41, 35.52. FTIR (neat, cm^{-1}) 2075. HRMS (EI) calcd for $C_{12}H_{11}N_3$, 197.0950; found, 197.0952.

Azides **B37**, **B39**, and **B40** were prepared from the corresponding alcohols using the same procedure described for **B35**.

*3-(2-Azidoethyl)thiophene (**B37**).* Yield 84%; a colorless oil. ^1H NMR ($CDCl_3$, 500 MHz, δ; ppm): 7.29 (1H, m), 7.06 (1H, d, J = 1.8 Hz), 6.98 (1H, d, J = 4.3 Hz), 3.51 (2H, t, J = 7.0 Hz), 2.93 (2H, t, J = 7.0 Hz). ^{13}C NMR ($CDCl_3$, 150 MHz, δ; ppm): 138.26, 127.97, 125.95, 121.79, 51.79, 29.81. FTIR (neat, cm^{-1}) 2086. MS (EI) m/z 125 ($M^+ - 28$).

*5-(2-Azidoethyl)-4-methylthiazole (**B39**).* Yield 86%; a colorless oil. ^1H NMR ($CDCl_3$, 500 MHz, δ; ppm): 8.62 (1H, s), 3.51 (2H, t, J = 6.9 Hz), 3.04 (2H, t, J = 6.9 Hz), 2.43 (3H, s). ^{13}C NMR ($CDCl_3$, 125 MHz, δ; ppm): 150.06, 150.02, 127.01, 52.06, 26.27, 14.95. FTIR (neat, cm^{-1}) 2090. HRMS (EI) calcd for $C_6H_8N_4S$, 168.0473; found, 198.0475.

*4-(2-Azidoethyl)morpholine (**B40**).* Yield 50%; a yellow oil. ^1H NMR ($CDCl_3$, 500 MHz, δ; ppm): 3.73 (4H, t, J = 4.7 Hz), 3.35 (2H,

dx.doi.org/10.1021/jm300837y | J. Med. Chem. 2012, 55, 9562−9575

t, J = 5.9 Hz), 2.60 (2H, t, J = 5.9 Hz), 2.51 (4H, t, J = 4.6 Hz). ^{13}C NMR ($CDCl_3$, 125 MHz, δ; ppm): 66.91, 57.63, 53.62, 47.94. FTIR (neat, cm^{-1}) 2094.

*2-(2-Azidoethyl)pyridine (**B38**).* To a solution of 2-pyridineethanol (**27c**, 1.10 g, 8.93 mmol) and CBr_4 (3.26 g, 9.83 mmol) in CH_2Cl_2 (10 mL) was added a solution of PPh_3 (2.58 g, 9.83 mmol) in CH_2Cl_2 (5 mL) at 0 °C, and the mixture was stirred for 1 h at room temperature and then concentrated in vacuo. Purification of the residue by silica gel flash column chromatography (AcOEt/*n*-hexane = 1/4) gave 596 mg (36%) of the bromide as a colorless oil. To a 0.5 M solution of NaN_3 in DMSO (7.68 mL, 3.84 mmmol) was added the bromide (596 mg, 3.20 mmol), and the mixture was stirred at room temperature for 2 h. The reaction mixture was poured into water and extracted with AcOEt. The AcOEt layer was washed with water and brine and dried over Na_2SO_4. Filtration, concentration in vacuo, and purification of the residue by silica gel flash column chromatography (AcOEt/*n*-hexane = 1/3) gave 207 mg (44%) of **B38** as a pale-yellow oil. ^{1}H NMR ($CDCl_3$, 500 MHz, δ; ppm): 8.57 (1H, d, J = 4.3 Hz), 7.64 (1H, dt, J = 1.5, 7.6 Hz), 7.21−7.16 (2H, m), 3.72 (2H, t, J = 7.0 Hz), 3.06 (2H, t, J = 7.0 Hz). ^{13}C NMR ($CDCl_3$, 150 MHz, δ; ppm): 158.04, 149.60, 136.55, 123.57, 121.84, 50.70, 37.52. FTIR (neat, cm^{-1}) 2090. MS (EI) m/z 119 (M^+ − 28).

*(E)-(2-Azidovinyl)benzene (**B46**).* To a solution of $CuSO_4$ (118 mg, 0.737 mmol) and NaN_3 (575 mg, 8.84 mmol) in MeOH (20 mL) was added (*E*)-2-phenylvinylboronic acid (**30**, 1.09 g, 7.37 mmol), and the mixture was stirred for 30 h at room temperature. After removal of the solvent, the residue was diluted with AcOEt. The AcOEt solution was washed water and brine and dried over Na_2SO_4. Filtration, concentration in vacuo, and purification of the residue by silica gel flash column chromatography (AcOEt/*n*-hexane = 1/10) gave 425 mg (40%) of **B46** as a yellow oil. ^{1}H NMR ($CDCl_3$, 500 MHz, δ; ppm): 7.32−7.20 (5H, m), 6.61 (1H, d, J = 14 Hz), 6.27 (1H, d, J = 14 Hz). ^{13}C NMR ($CDCl_3$, 125 MHz, δ; ppm): 135.02, 128.76, 127.39, 126.68, 125.82, 119.80. FTIR (neat, cm^{-1}) 2090, 1635. HRMS (EI) calcd for $C_8H_7N_3$, 145.0644; found, 145.0645.

Construction of a 120-Member Triazole Library (C1−C120) and a 31-Member Triazole Library (C121−C151). To a solution of an alkyne (25 mM, 20 μL), an azide (30 mM, 20 μL), and TBTA (5 mM, 10 μL) in DMSO was added an aqueous solution of $CuSO_4{\cdot}5H_2O$ (2 mM, 25 μL) on a 96-well plate. To the resulting mixture was added an aqueous solution of sodium ascorbate (10 mM, 25 μL), and the mixture was shaken for 1−3 days at room temperature. The reaction was monitored by TLC and LCMS. When the reaction was completed, DMSO (150 μL) was added to the mixture, in which the concentration of the triazole is assumed to be 2 mM. The crude triazoles were diluted to a desired concentration for enzyme assays.

*3-(1-Benzyl-1H-[1,2,3]triazol-4-yl)-1-carboxylic Acid Hydroxyamide (**C31**).* To a solution of **A3** (43.2 mg, 0.268 mmol), **B1** (51.8 mg, 0.322 mmol), and TBTA (14.2 mg, 10 mol %) in MeOH (5 mL) was added a solution of $CuSO_4{\cdot}5H_2O$ (6.69 mg, 10 mol %) and sodium ascorbate (26.5 mg, 50 mol %) in water (5 mL). The reaction mixture was stirred for 24 h at room temperature and then poured into water and extracted with AcOEt. The AcOEt layer was separated, washed with water and brine, and dried over Na_2SO_4. Filtration, concentration in vacuo, and purification of the residue by silica gel flash column chromatography (AcOEt/*n*-hexane = 2/1) gave 82.2 mg (q.y.) of **C31** as a pale-yellow solid. The solid was recrystallized from MeOH to give 40.9 mg of **C31** as colorless crystals; mp 154−155 °C. ^{1}H NMR (DMSO-d_6, 600 MHz, δ; ppm): 11.3 (1H, broad s), 9.08 (1H, s) 8.69 (1H, s), 8.23 (1H, t, J = 1.6 Hz), 7.98 (1H, d, J = 7.7 Hz), 7.69 (1H, dt, J = 1.4, 7.9 Hz), 7.52 (1H, t, J = 7.7 Hz), 7.42−7.34 (5H, m), 5.67 (2H, s). ^{13}C NMR (DMSO-d_6, 125 MHz, δ; ppm): 163.93, 146.07, 135.89, 133.45, 130.80, 128.99, 128.79, 128.18, 127.93, 127.63, 126.18, 123.73, 121.90, 53.06. MS (FAB) m/z 295 (MH^+). Anal. ($C_{16}H_{14}N_4O_2{\cdot}H_2O$) C, H, N.

Compounds **C32**, **C142**, and **C149** were prepared from **A3** and the corresponding azides using the same procedure described for **C31**.

*3-(1-Phenethyl-1H-[1,2,3]triazol-4-yl)-1-carboxylic Acid Hydroxyamide (**C32**).* Yield 92%; colorless crystals; mp 168−170 °C. ^{1}H NMR (DMSO-d_6, 600 MHz, δ; ppm): 11.3 (1H, broad s), 9.08 (1H, s) 8.59 (1H, s), 8.20 (1H, d, J = 1.6 Hz), 7.93 (1H, d, J = 7.7 Hz), 7.68 (1H, dt, J = 1.2, 6.5 Hz), 7.52 (1H, t, J = 7.7 Hz), 7.30−7.20 (5H, m), 4.68 (2H, t, J = 7.3 Hz), 3.23 (2H, t, J = 7.3 Hz). ^{13}C NMR (DMSO-d_6, 125 MHz, δ; ppm): 163.98, 145.53, 137.56, 133.49, 130.96, 128.99, 128.65, 128.41, 127.54, 126.58, 126.03, 123.68, 121.90, 50.65, 35.49. MS (FAB) m/z 309 (MH^+). Anal. ($C_{17}H_{16}N_4O_2{\cdot}H_2O$) C, H, N.

*N-Hydroxy-3-[1-(2-thiophen-3-yl-ethyl)-1H-[1,2,3]triazol-4-yl]-benzamide (**C142**).* Yield 100%; colorless crystals; mp 164−166 °C. ^{1}H NMR (DMSO-d_6, 500 MHz, δ; ppm): 11.3 (1H, broad s), 9.09 (1H, s) 8.59 (1H, s), 8.21 (1H, s), 7.94 (1H, d, J = 7.6 Hz), 7.68 (1H, d, J = 7.9 Hz), 7.52 (1H, t, J = 7.6 Hz), 7.48−7.46 (1H, m), 7.24 (1H, s), 7.00 (1H, d, J = 4.8 Hz), 4.67 (2H, t, J = 7.3 Hz), 3.25 (2H, t, J = 7.3 Hz). ^{13}C NMR (DMSO-d_6, 150 MHz, δ; ppm): 163.88, 145.47, 137.68, 133.40, 130.89, 128.93, 128.11, 127.48, 126.12, 125.95, 123.62, 122.01, 121.59, 49.94, 30.08. MS (FAB) m/z 315 (MH^+). Anal. ($C_{15}H_{14}N_4O_2S$) C, H, N.

*N-Hydroxy-3-(1-phenylsulfanylmethyl-1H-[1,2,3]triazol-4-yl)-benzamide (**C149**).* Yield 92%; colorless crystals; mp 160−161 °C. ^{1}H NMR (DMSO-d_6, 500 MHz, δ; ppm): 11.3 (1H, broad s), 9.09 (1H, s) 8.63 (1H, s), 8.21 (1H, t, J = 1.5 Hz), 7.96 (1H, d, J = 7.9 Hz), 7.70 (1H, dt, J = 1.2, 7.6 Hz), 7.52 (1H, t, J = 7.9 Hz), 7.45−7.43 (2H, m), 7.37−7.30 (3H, m), 6.01 (2H, s). ^{13}C NMR (DMSO-d_6, 125 MHz, δ; ppm): 163.87, 146.10, 133.47, 132.27, 130.66, 130.52, 129.31, 129.06, 127.79, 127.70, 126.35, 123.71, 121.37, 52.02. MS (FAB) m/z 327 (MH^+). Anal. ($C_{16}H_{14}N_4O_2S$) C, H, N.

Biology. *Enzyme Assays.* The HDAC activity assay was performed using an HDACs/HDAC8 deacetylase fluorometric assay kit (CY-1150/CY-1158, Cyclex Company Limited), HDAC1/HDAC6 fluorescent activity drug discovery kit (AK-511/AK-516, BIOMOL Research Laboratories), fluorescent SIRT1 activity assay/drug discovery kit (AK-555, BIOMOL Research Laboratories), or fluorogenic HDAC class 2α assay kit (BPS Bioscience Incorporated) with HDACs (CY-1150, Cyclex Company Limited), HDAC1 (SE-456, BIOMOL Research Laboratories), HDAC2 (SE-500, BIOMOL Research Laboratories), HDAC4 (BPS Bioscience Incorporated), HDAC6 (SE-508, BIOMOL Research Laboratories), and HDAC8 (CY-1158, Cyclex Company Limited), according to the supplier's instructions. The fluorescence of the wells was measured on a fluorometric reader with excitation set at 360 nm and emission detection set at 460 nm, and the % inhibition was calculated from the fluorescence readings of inhibited wells relative to those of control wells. The concentration of a compound that results in 50% inhibition (IC_{50}) was determined by plotting log[Inh] versus the logit function of % inhibition. IC_{50} values were determined by regression analysis of the concentration/inhibition data. For determination of IC_{50} values, various concentrations (0.0001, 0.001, 0.01, 0.1, 1.0, 10, and 100 μM) of inhibitors were used.

Cell Growth Inhibition Assay. The cells were plated at the initial density of 2×10^5 cells/well (50 μL/well) in 96-well plates in medium culture and exposed to inhibitors for 72 h at 37 °C in 5% CO_2 incubator. A solution of 3-(4,5-dimethylthiazol-2-yl)-5-(3-carboxymethoxyphenyl)-2-(4-sulfophenyl)-2*H*-tetrazolium, inner salt (MTS) was then added (20 μL/well), and incubation was continued for 2 h. The solubilized dye was quantified by colorimetric reading at 490 nm using a reference wavelength of 650 nm. The absorbance values of control wells (C) and test wells (T) were measured. The absorbance of the test wells (T_0) was also measured at time 0 (addition of compounds). Using these measurements, cell growth inhibition (percentage of growth) by a test inhibitor at each concentration used was calculated as: % growth = $100[(T - T_0)/(C - T_0)]$, when $T > T_0$ and % growth = $100[(T - T_0)/T]$, when $T < T_0$. Computer analysis of the % growth values afforded the 50% growth inhibition parameter (GI_{50}). The GI_{50} was calculated as $100[(T - T_0)/(C - T_0)] = 50$.

Western Blot Analysis. The cohesin- or H4-acetylating activities of the test compounds were assayed according to the method reported in ref 24.

Molecular Modeling. The X-ray structure of HDAC8 (PDB code 1VKG) was used as the target structure for docking. Protein preparation, receptor grid generation, and ligand docking were

dx.doi.org/10.1021/jm300837y | J. Med. Chem. 2012, 55, 9562−9575

performed using the software Glide 3.5. Compounds **C149** and **6** were docked into the ligand binding site of HDAC8. The standard precision mode of Glide was used to determine favorable binding poses, which allowed the ligand conformation to be flexibly explored while holding the protein as a rigid structure during docking. Then, the predicted complex structure was fully energy-minimized, with both the protein and the ligand allowed to move, using Macromodel 8.1 software. The conformation of compounds **C149** and **6** in the ligand binding site was minimized by MM calculation based on the OPLS-AA force field with the following parameter set: solvent, water; method, LBFGS; max no. of iterations, 10000; converge, gradient; convergence threshold, 0.05.

■ ASSOCIATED CONTENT

Supporting Information

Results of LCMS analysis of representative compounds, the 120-member triazole library for HDAC inhibitors obtained by the combination of alkynes **A1**−**A8** and azides **B1**−**B15**, the 31-member **C32**-based library for HDAC8-selective inhibitors obtained by the combination of alkyne **A3** and azides **B16**−**B46**, and results of elemental analysis of **A3**−**A8**, **C31**, **C32**, **C142**, and **C149** are reported. This material is available free of charge via the Internet at http://pubs.acs.org.

■ AUTHOR INFORMATION

Corresponding Author

*Phone/Fax: +81-52-836-3407. E-mail: suzukit@koto.kpu-m.ac.jp (T.S.); miyata-n@phar.nagoya-cu.ac.jp (N.M.).

Notes

The authors declare no competing financial interest.

■ ACKNOWLEDGMENTS

We thank Mie Tsuchida for her technical support. This work was supported in part by JST PRESTO program (T.S.), a Grant-in-Aid for Scientific Research from the JapanSociety for the Promotion of Science (T.S.), Foundation NAGASE Science Technology Development (T.S.), and the Shorai Foundation for Science and Technology (T.S.).

■ ABBREVIATIONS USED

HDAC, histone deacetylase; SIRT, sirtuin; TSA, trichostatin A; CuAAC, Cu(I)-catalyzed azide−alkyne cycloaddition; ZBG, zinc-binding group; TBTA, tris[(1-benzyl-1*H*-1,2,3-triazol-4-yl)methyl]amine; SMC, structural maintenance of chromosome; PBMC, peripheral blood mononuclear cell

■ REFERENCES

(1) (a) Grozinger, C. M.; Schreiber, S. L. Deacetylase enzymes: Biological functions and the use of small-molecule inhibitors. *Chem. Biol.* **2002**, *9*, 3−16. (b) Yoshida, M.; Shimazu, T.; Matsuyama, A. Protein deacetylases: enzymes with functional diversity as novel therapeutic targets. *Prog. Cell Cycle Res.* **2003**, *5*, 269−278. (c) Glozak, M. A.; Sengupta, N.; Zhang, X.; Seto, E. Acetylation and deacetylation of non-histone proteins. *Gene* **2005**, *363*, 15−23. (d) Konstantinopoulos, P. A.; Karamouzis, M. V.; Papavassiliou, A. G. Focus on acetylation: the role of histone deacetylase inhibitors in cancer therapy and beyond. *Expert Opin. Invest. Drugs* **2007**, *16*, 569−571.

(2) (a) Biel, M.; Wascholowski, V.; Giannis, A. Epigenetics—an epicenter of gene regulation: histones and histone-modifying enzymes. *Angew. Chem., Int. Ed.* **2005**, *44*, 3186−3216. (b) Mai, A.; Massa, S.; Rotili, D.; Cerbara, I.; Valente, S.; Pezzi, R.; Simeoni, S.; Ragno, R. Histone deacetylation in epigenetics: an attractive target for anticancer therapy. *Med. Res. Rev.* **2005**, *25*, 261−309. (c) Suzuki, T.; Miyata, N. Epigenetic control using natural products and synthetic molecules. *Curr. Med. Chem.* **2006**, *13*, 935−958. (d) Schaefer, S.; Jung, M. Chromatin modifications as targets for new anticancer drugs. *Arch. Pharm.* **2005**, *338*, 347−357. (e) Itoh, Y.; Suzuki, T.; Miyata, N. Isoform-selective histone deacetylase inhibitors. *Curr. Pharm. Des.* **2008**, *14*, 529−544.

(3) (a) Hu, E.; Chen, Z.; Fredrickson, T.; Zhu, Y.; Kirkpatrick, R.; Zhang, G. F.; Johanson, K.; Sung, C. M.; Liu, R.; Winkler, J. Cloning and characterization of a novel human class I histone deacetylase that functions as a transcription repressor. *J. Biol. Chem.* **2000**, *275*, 15254−15264. (b) Buggy, J. J.; Sideris, M. L.; Mak, P.; Lorimer, D. D.; McIntosh, B.; Clark, J. M. Cloning and characterization of a novel human histone deacetylase, HDAC8. *Biochem. J.* **2000**, *350*, 199−205. (c) Nakagawa, M.; Oda, Y.; Eguchi, T.; Aishima, S.; Yao, T.; Hosoi, F.; Basaki, Y.; Ono, M.; Kuwano, M.; Tanaka, M.; Tsuneyoshi, M. Expression profile of class I histone deacetylases in human cancer tissues. *Oncol. Rep.* **2007**, *18*, 769−774.

(4) Waltregny, D.; De Leval, L.; Glénisson, W.; Ly Tran, S.; North, B. J.; Bellahcène, A.; Weidle, U.; Verdin, E.; Castronovo, V. Expression of histone deacetylase 8, a class I histone deacetylase, is restricted to cells showing smooth muscle differentiation in normal human tissues. *Am. J. Pathol.* **2004**, *165*, 553−564.

(5) Durst, K. L.; Lutterbach, B.; Kummalue, T.; Friedman, A. D.; Hiebert, S. W. The inv(16) fusion protein associates with corepressors via a smooth muscle myosin heavy-chain domain. *Mol. Cell. Biol.* **2003**, *23*, 607−619.

(6) Waltregny, D.; Glénisson, W.; Ly Tran, S.; North, B. J.; Verdin, E.; Colige, A.; Castronovo, V. Histone deacetylase HDAC8 associates with smooth muscle alpha-actin and is essential for smooth muscle cell contractility. *FASEB J.* **2005**, *19*, 966−968.

(7) Gallinari, P.; Di Marco, S.; Jones, P.; Pallaoro, M.; Steinkühler, C. HDACs, histone deacetylation and gene transcription: from molecular biology to cancer therapeutics. *Cell Res.* **2007**, *17*, 195−211.

(8) Balasubramanian, S.; Ramos, J.; Luo, W.; Sirisawad, M.; Verner, E.; Buggy, J. J. A novel histone deacetylase 8 (HDAC8)-specific inhibitor PCI-34051 induces apoptosis in T-cell lymphomas. *Leukemia* **2008**, *22*, 1026−1034.

(9) Oehme, I.; Deubzer, H. E.; Wegener, D.; Pickert, D.; Linke, J. P.; Hero, B.; Kopp-Schneider, A.; Westermann, F.; Ulrich, S. M.; von Deimling, A.; Fischer, M.; Witt, O. Histone deacetylase 8 in neuroblastoma tumorigenesis. *Clin. Cancer Res.* **2009**, *15*, 91−99.

(10) (a) Miller, T. A.; Witter, D. J.; Belvedere, S. Histone deacetylase inhibitors. *J. Med. Chem.* **2003**, *46*, 5097−5116. (b) Paris, M.; Porcelloni, M.; Binaschi, M.; Fattori, D. Histone deacetylase inhibitors: from bench to clinic. *J. Med. Chem.* **2008**, *51*, 1505−1529. (c) Suzuki, T.; Nagano, Y.; Kouketsu, A.; Matsuura, A.; Maruyama, S.; Kurotaki, M.; Nakagawa, H.; Miyata, N. Novel inhibitors of human histone deacetylases: Design, synthesis, enzyme inhibition, and cancer cell growth inhibition of SAHA-based non-hydroxamates. *J. Med. Chem.* **2005**, *48*, 1019−1032. (d) Suzuki, T.; Kouketsu, A.; Itoh, Y.; Hisakawa, S.; Maeda, S.; Yoshida, M.; Nakagawa, H.; Miyata, N. Highly potent and selective histone deacetylase 6 inhibitors designed based on a small-molecular substrate. *J. Med. Chem.* **2006**, *49*, 4809−4812. (e) Itoh, Y.; Suzuki, T.; Kouketsu, A.; Suzuki, N.; Maeda, S.; Yoshida, M.; Nakagawa, H.; Miyata, N. Design, synthesis, structure−selectivity relationship, and effect on human cancer cells of a novel series of histone deacetylase 6-selective inhibitors. *J. Med. Chem.* **2007**, *50*, 5425−5438. (f) Suzuki, N.; Suzuki, T.; Ota, Y.; Nakano, T.; Kurihara, M.; Okuda, H.; Yamori, T.; Tsumoto, H.; Nakagawa, H.; Miyata, N. Design, synthesis, and biological activity of boronic acid-based histone deacetylase inhibitors. *J. Med. Chem.* **2009**, *52*, 2909−2922.

(11) (a) Yoshida, M.; Kijima, M.; Akita, M.; Beppu, T. Potent and specific inhibition of mammalian histone deacetylase both in vivo and in vitro by Trichostatin A. *J. Biol. Chem.* **1990**, *265*, 17174−17179. (b) Yoshida, M.; Horinouchi, S.; Beppu, T. Trichostatin A and trapoxin: novel chemical probes for the role of histone acetylation in chromatin structure and function. *BioEssays* **1995**, *17*, 423−430.

(12) (a) Richon, V. M.; Emiliani, S.; Verdin, E.; Webb, Y.; Breslow, R.; Rifkind, R. A.; Marks, P. A. A class of hybrid polar inducers of transformed cell differentiation inhibits histone deacetylases. *Proc. Natl. Acad. Sci. U. S. A.* **1998**, *95*, 3003−3007. (b) Richon, V. M.;

Webb, Y.; Merger, R.; Sheppard, T.; Jursic, B.; Ngo, L.; Civoli, F.; Breslow, R.; Rifkind, R. A.; Marks, P. A. Second generation hybrid polar compounds are potent inducers of transformed cell differentiation. *Proc. Natl. Acad. Sci. U. S. A.* **1996**, *93*, 5705−5708.

(13) Suzuki, T.; Ando, T.; Tsuchiya, K.; Fukazawa, N.; Saito, A.; Mariko, Y.; Yamashita, T.; Nakanishi, O. Synthesis and histone deacetylase inhibitory activity of new benzamide derivatives. *J. Med. Chem.* **1999**, *42*, 3001−3003.

(14) Hu, E.; Dul, E.; Sung, C. M.; Chen, Z.; Kirkpatrick, R.; Zhang, G. F.; Johanson, K.; Liu, R.; Lago, A.; Hofmann, G.; Macarron, R.; de los Frailes, M.; Perez, P.; Krawiec, J.; Winkler, J.; Jaye, M. Identification of novel isoform-selective inhibitors within class I histone deacetylases. *J. Pharmacol. Exp. Ther.* **2003**, *307*, 720−728.

(15) KrennHrubec, K.; Marshall, B. L.; Hedglin, M.; Verdin, E.; Ulrich, S. M. Design and evaluation of 'Linkerless' hydroxamic acids as selective HDAC8 inhibitors. *Bioorg. Med. Chem. Lett.* **2007**, *17*, 2874−2878.

(16) Whitehead, L.; Dobler, M. R.; Radetich, B.; Zhu, Y.; Atadja, P. W.; Claiborne, T.; Grob, J. E.; McRiner, A.; Pancost, M. R.; Patnaik, A.; Shao, W.; Shultz, M.; Tichkule, R.; Tommasi, R. A.; Vash, B.; Wang, P.; Stams, T. Human HDAC isoform selectivity achieved via exploitation of the acetate release channel with structurally unique small molecule inhibitors. *Bioorg. Med. Chem.* **2011**, *19*, 4626−4634.

(17) Tang, W.; Luo, T.; Greenberg, E. F.; Bradner, J. E.; Schreiber, S. L. Discovery of histone deacetylase 8 selective inhibitors. *Bioorg. Med. Chem. Lett.* **2011**, *21*, 2601−2605.

(18) (a) Kolb, H. C.; Finn, M. G.; Sharpless, K. B. Click Chemistry: Diverse Chemical Function from a Few Good Reactions. *Angew. Chem., Int. Ed.* **2001**, *40*, 2004−2021. (b) Hein, J. E.; Krasnova, L. B.; Iwasaki, M.; Fokin, V. V. Cu-Catalyzed azide-alkyne cycloaddition: preparation of tris((1-benzyl-1*H*-1,2,3-triazolyl)mehtyl)amine. *Org. Synth.* **2011**, *88*, 238−247.

(19) (a) Suzuki, T.; Ota, Y.; Kasuya, Y.; Mutsuga, M.; Kawamura, Y.; Tsumoto, H.; Nakagawa, H.; Finn, M. G.; Miyata, N. An unexpected example of protein-templated click chemistry. *Angew. Chem., Int. Ed.* **2010**, *49*, 6817−6820. (b) Hou, J.; Feng, C.; Li, Z.; Fang, Q.; Wang, H.; Gu, G.; Shi, Y.; Liu, P.; Xu, F.; Yin, Z.; Shen, J.; Wang, P. Structure-based optimization of click-based histone deacetylase inhibitors. *Eur. J. Med. Chem.* **2011**, *46*, 3190−3200. (c) Shen, J.; Woodward, R.; Kedenburg, J. P.; Liu, X.; Chen, M.; Fang, L.; Sun, D.; Wang, P. G. Histone deacetylase inhibitors through click chemistry. *J. Med. Chem.* **2008**, *51*, 7417−7427. (d) Chen, P. C.; Patil, V.; Guerrant, W.; Green, P.; Oyelere, A. K. Synthesis and structure−activity relationship of histone deacetylase (HDAC) inhibitors with triazole-linked cap group. *Bioorg. Med. Chem.* **2008**, *16*, 4839−4853.

(20) Arkin, M. R.; Wells, J. A. Small-molecule inhibitors of protein−protein interactions: progressing towards the dream. *Nature Rev. Drug. Discovery* **2004**, *3*, 301−317.

(21) (a) Lee, L. V.; Mitchell, M. L.; Huang, S. J.; Fokin, V. V.; Sharpless, K. B.; Wong, C. H. A potent and highly selective inhibitor of human α-1,3-fucosyltransferase via click chemistry. *J. Am. Chem. Soc.* **2003**, *125*, 9588−9589. (b) Srinivasan, R.; Uttamchandani, M.; Yao, S. Q. Rapid assembly and in situ screening of bidentate inhibitors of protein tyrosine phosphatases. *Org. Lett.* **2006**, *8*, 713−716. (c) Wang, J.; Uttamchandani, M.; Li, J.; Hu, M.; Yao, S. Q. Rapid assembly of matrix metalloprotease inhibitors using click chemistry. *Org. Lett.* **2006**, *8*, 3821−3824. (d) Srinivasan, R.; Li, J.; Ng, S. L.; Kalesh, K. A.; Yao, S. Q. Methods of using click chemistry in the discovery of enzyme inhibitors. *Nat. Protoc.* **2007**, *2*, 2655−2664. (e) Hu, M.; Li, J.; Yao, S. Q. In situ "click" assembly of small molecule matrix metalloprotease inhibitors containing zinc-chelating groups. *Org. Lett.* **2008**, *10*, 5529−5531. (f) Tan, L. P.; Wu, H.; Yang, P. Y.; Kalesh, K. A.; Zhang, X.; Hu, M.; Srinivasan, R.; Yao, S. Q. High-throughput discovery of *Mycobacterium tuberculosis* protein tyrosine phosphatase B (MptpB) inhibitors using click chemistry. *Org. Lett.* **2009**, *11*, 5102−5105.

(22) (a) Rostovtsev, V. V.; Green, L. G.; Fokin, V. V.; Sharpless, K. B. A stepwise huisgen cycloaddition process: copper(I)-catalyzed regioselective "ligation" of azides and terminal alkynes. *Angew. Chem., Int. Ed.* **2002**, *41*, 2596−2599. (b) Tornøe, C. W.; Christensen, C.; Meldal, M. Peptidotriazoles on solid phase: [1,2,3]-triazoles by regiospecific copper(I)-catalyzed 1,3-dipolar cycloadditions of terminal alkynes to azides. *J. Org. Chem.* **2002**, *67*, 3057−3064.

(23) (a) Somoza, J. R.; Skene, R. J.; Katz, B. A.; Mol, C.; Ho, J. D.; Jennings, A. J.; Luong, C.; Arvai, A.; Buggy, J. J.; Chi, E.; Tang, J.; Sang, B.-C.; Verner, E; Wynands, R.; Leahy, E. M.; Dougan, D. R.; Snell, G.; Navre, M.; Knuth, M. W.; Swanson, R. V.; McRee, D. E.; Tari, L. W. Structural snapshots of human HDAC8 provide insights into the class I histone deacetylases. *Structure* **2004**, *12*, 1325−1334. (b) Vannini, A.; Volpari, C.; Filocamo, G.; Casavola, E. C.; Brunetti, M.; Renzoni, D.; Chakravarty, P.; Paolini, C.; De Francesco, R.; Gallinari, P.; Steinkühler, C.; Di Marco, S. Crystal structure of a eukaryotic zinc-dependent histone deacetylase, human HDAC8, complexed with a hydroxamic acid inhibitor. *Proc. Natl. Acad. Sci. U. S. A.* **2004**, *101*, 15064−15069. (c) Vannini, A.; Volpari, C.; Gallinari, P.; Jones, P.; Mattu, M.; Carfí, A.; De Francesco, R.; Steinkühler, C.; Di Marco, S. Substrate binding to histone deacetylases as shown by the crystal structure of the HDAC8−substrate complex. *EMBO Rep.* **2007**, *8*, 879−884. (d) Dowling, D. P.; Gantt, S. L.; Gattis, S. G.; Fierke, C. A.; Christianson, D. W. Structural studies of human histone deacetylase 8 and its site-specific variants complexed with substrate and inhibitors. *Biochemistry* **2008**, *47*, 13554−13563. (e) Dowling, D. P.; Gattis, S. G.; Fierke, C. A.; Christianson, D. W. Structures of metal-substituted human histone deacetylase 8 provide mechanistic inferences on biological function. *Biochemistry* **2010**, *49*, 5048−5056. (f) Cole, K. E.; Dowling, D. P.; Boone, M. A.; Phillips, A. J.; Christianson, D. W. Structural basis of the antiproliferative activity of largazole, a depsipeptide inhibitor of the histone deacetylases. *J. Am. Chem. Soc.* **2011**, *133*, 12474−12477.

(24) Bressi, J. C.; Jennings, A. J.; Skene, R.; Wu, Y.; Melkus, R.; De Jong, R.; O'Connell, S.; Grimshaw, C. E.; Navre, M.; Gangloff, A. R. Exploration of the HDAC2 foot pocket: synthesis and SAR of substituted *N*-(2-aminophenyl)benzamides. *Bioorg. Med. Chem. Lett.* **2010**, *20*, 3142−3145.

(25) Deardorff, M. A.; Bando, M.; Nakato, R.; Itoh, T.; Minamino, M.; Saitoh, K.; Komata, M.; Katou, Y.; Clark, D.; Cole, K. E.; De Baere, E.; Decroos, C.; Ernst, S.; Francey, L.; Gyftodimou, Y.; Hirashima, K.; Hullings, M.; Ishikawa, Y.; Kaur, M.; Kiyono, T.; Lombardi, P. M.; Mortier, G. R.; Nozaki, N.; Petersen, M. B.; Seimiya, H.; Siu, V. M.; Suzuki, Y.; Takagaki, K.; Tyshchenko, N.; Wilde, J. J.; Willems, P. J.; Gillessen-Kaesbach, G.; Christianson, D. W.; Kaiser, F. J.; Jackson, L. G.; Hirota, T.; Krantz, I. D.; Shirahige, K. HDAC8 mutations in Cornelia de Lange Syndrome affect the cohesin acetylation cycle. *Nature* **2012**, *489*, 313−317.

(26) Benati, L.; Bencivenni, G.; Leardini, R.; Nanni, D.; Minozzi, M.; Spagnolo, P.; Scialpi, R.; Zanardi, G. Reaction of azides with dichloroindium hydride: very mild production of amines and pyrrolidin-2-imines through possible indium-aminyl radicals. *Org. Lett.* **2006**, *8*, 2499−2502.

(27) Colombano, G.; Travelli, C.; Galli, U.; Caldarelli, A.; Chini, M. G.; Canonico, P. L.; Sorba, G.; Bifulco, G.; Tron, G. C.; Genazzani, A. A. A novel potent nicotinamide phosphoribosyltransferase inhibitor synthesized via click chemistry. *J. Med. Chem.* **2010**, *53*, 616−623.

(28) Sirion, U.; Kim, H. J.; Lee, J. H.; Seo, J. W.; Lee, B. S.; Lee, S. J.; Oh, S. J.; Chi, D. Y. An efficient F-18 labeling method for PET study: Huisgen 1,3-dipolar cycloaddition of bioactive substances and F-18-labeled compounds. *Tetrahedron Lett.* **2007**, *48*, 3953−3957.

(29) Papeo, G.; Posteri, H.; Vianello, P.; Varasi, M. Nicotinoyl azide (NCA)-mediated Mitsunobu reaction: an expedient one-pot transformation of alcohols into azides. *Synthesis* **2004**, 2886−2892.

(30) Goto, R.; Okura, K.; Sakazaki, H.; Sugawara, T.; Matsuoka, S.; Inoue, M. Synthesis and biological evaluation of triazole analogues of antillatoxin. *Tetrahedron* **2011**, *67*, 6659−6672.